Hydrol. Earth Syst. Sci. Discuss., 11, 9219–9279, 2014
www.hydrol-earth-syst-sci-discuss.net/11/9219/2014/
doi:10.5194/hessd-11-9219-2014

Hydrology and Earth System Sciences
Discussions
Open Access

An integrated water system model considering hydrological and biogeochemical processes at basin scale: model construction and application

Y. Y. Zhang[1,2], Q. X. Shao[2], A. Z. Ye[3], and H. T. Xing[1,4]

[1]Key Laboratory of Water Cycle and Related Land Surface Processes, Institute of Geographic Sciences and Natural Resources Research, Chinese Academy of Sciences, Beijing, 100101, China
[2]CSIRO Digital Productivity and Services Flagship, Leeuwin Centre, 65 Brockway Road, Floreat Park, WA 6014, Australia
[3]College of Global Change and Earth System Science, Beijing Normal University, Beijing, 100875, China
[4]CSIRO Agriculture Flagship, GPO Box 1666, Canberra, ACT2601, Australia

Received: 14 July 2014 – Accepted: 21 July 2014 – Published: 4 August 2014

Correspondence to: Y. Y. Zhang (zhangyy003@gmail.com)
and Q. X. Shao (quanxi.shao@cisro.au)

Published by Copernicus Publications on behalf of the European Geosciences Union.

Abstract

Integrated water system modeling is a reasonable approach to provide scientific understanding and possible solutions to tackle the severe water crisis faced over the world and to promote the implementation of integrated river basin management. Such a modeling practice becomes more feasible nowadays due to better computing facilities and available data sources. In this study, the process-oriented water system model (HE^XM) is developed by integrating multiple water related processes including hydrology, biogeochemistry, environment and ecology, as well as the interference of human activities. The model was tested in the Shaying River Catchment, the largest, highly regulated and heavily polluted tributary of Huai River Basin in China. The results show that: HE^XM is well integrated with good performance on the key water related components in the complex catchments. The simulated daily runoff series at all the regulated and less-regulated stations matches observations, especially for the high and low flow events. The average values of correlation coefficient and coefficient of efficiency are 0.81 and 0.63, respectively. The dynamics of observed daily ammonia-nitrogen (NH_4-N) concentration, as an important index to assess water environmental quality in China, are well captured with average correlation coefficient of 0.66. Furthermore, the spatial patterns of nonpoint source pollutant load and grain yield are also simulated properly, and the outputs have good agreements with the statistics at city scale. Our model shows clear superior performance in both calibration and validation in comparison with the widely used SWAT model. This model is expected to give a strong reference for water system modeling in complex basins, and provide the scientific foundation for the implementation of integrated river basin management all over the world as well as the technical guide for the reasonable regulation of dams and sluices and environmental improvement in river basins.

HESSD
11, 9219–9279, 2014

1 Introduction

Severe water crisis is a global issue including flooding (Milly et al., 2002; Schiermeier et al., 2011), water shortages (Pimentel et al., 2004; Wilhite et al., 2005), water pollution (Jordan et al., 2014; Zhou et al., 2014) and ecological degradation (Revenga et al., 2000; Vörösmarty et al., 2010), which have hindered sustainable development in many regions over the world. It is widely agreed that it is impossible to solve these water problems using only the traditional hydrological method because of the interconnections between water and other related eco-environment in the complicated water system (Kindler, 2000). The process-oriented water system model is one of the most sensible and efficient tools to address these problems and promote the application of integrated river basin management.

The hydrological cycle has been widely accepted as a critical linkage among physical (e.g. runoff, energy), biogeochemical (e.g. nutrient, water quality) and ecological processes (e.g. plant growth), energy process at basin scale (Wigmosta et al., 1994; Singh et al., 2002; Burt and Pinay, 2005). For example, the physiological and ecological processes of vegetation affect the evapotranspiration, soil moisture distribution and infiltration in the major components of water cycle, and the nutrients absorption and movement in the biochemical cycle. On the contrary, soil moisture in the hydrological process and nutrient content in the biochemical processes directly affects crop growth through physiological and ecological processes of vegetation within the plant. The overland flow in the hydrological process affects the pollutant load discharge to water body in the environmental processes. Therefore, it is more reasonable to assess the impact of climate change or human activities at the basin scale and to achieve better river basin management by coupling these processes to capture the interaction and feedback between the individual cycles.

Multidisciplinary research provides a new way to solve highly complicated problems. This is particularly true when dealing with severe water crisis faced in water resources management. The water system modeling can be proposed to combine water-related disciplines (hydrology, environment and ecology, etc.) by including most of water-related processes. Furthermore, the basic theories of water-related disciplines have been formalized for over a century, such as accumulated temperature law for phenological development in 1735, Dacy's law for groundwater flow in 1856, Saint-Venant Equation for surface flow in 1871, balance equation for mass and momentum in 1915, Richards equation for unsaturated zone in 1931, Horton theory for infiltration in 1945, Penman–Monteith equation for evapotranspiration in 1965. These mature theories, when combined with advanced geospatial technologies (RS, GIS and GPS etc.) and high computer performance provide a scientific platform and support to make a new breakthrough of water system modeling at the macro-scale.

Since the 1980s, integrated water system modeling has always been one of the hot-topics in water science. Several models have been developed based on the mature models of different disciplines (hydrology, environment and ecology). Most existing models can be categorized into hydrology based, environment based, or biogeochemistry based models. Table 1 gives the components considered in several famous models. The hydrology based models extend the rainfall–runoff relationship to include the linkage with environmental and biogeochemical processes which however are usually weak and depicted by the empirical or black-box equations. As a result, the hydrology based models usually have satisfactory performance in hydrological process. Examples of widely accepted hydrology based models include HSPF (Bicknell et al., 1993), ANSWERS-Continuous (Bouraoui and Dillaha, 1996), AnnAGNPS (Bingner and Theurer, 2001). The environment based models depict the detail migration and transformation processes of pollutants in receiving water bodies using numerical solutions of one, two or three dimensional water dynamics equations. Thus the models are subject to computational instability and time consuming due to its complexity. The typical models are WASP (Di Toro et al., 1983), QUAL2K (Brown and Barnwell, 1987), EFDC (Hamrick, 1992). The biogeochemistry based models have advantages to simulate physiological and ecological processes of vegetation, the vertical movement of nutrients and water in soil layers at the field scale or experimental catchment scale, but

HESSD
11, 9219–9279, 2014

lack the accurate hydrological features (Deng et al., 2011). Thus it is hard to simulate the longitudinal movement of water and nutrients and their loss along flow path in the basin. The examples are EPIC (Sharpley and Williams, 1990), DNDC (Li et al., 1992). So far, SWAT is a typical integrated water system model, which simulates most of water related processes over long time periods at large scales and has been widely used all over the world (Arnold et al., 1998). However, the mechanism of each module in SWAT is over-simplified and conceptual described in its model setting.

Most of existing models focus on one or two major processes at the site or basin scale according to the major management objectives (e.g. flooding control, drought relief and pollution improvement) (Singh et al., 2002). However, none of the existing integrated models considered all the components, except abovementioned SWAT which however is over-simplified and only models long-term tendencies of processes (Neitsch et al., 2000). In practice, the traditional water resource management is transiting to integrated river basin management by considering runoff, water quality and ecological responses, as well as human water requirements (Gleick, 1998). This advanced management approach has prevailed since the beginning of this century in the world and has been gradually adopted in China.

However, new challenges are emerging in the integrated river basin management, such as the complicated interaction mechanism of water, geochemistry, ecology (Kirchner, 2003), the multiple scale problem (McDonnell et al., 2007), and the trade-off in allocating water resources among the living, production and ecology (Letcher et al., 2007). The models mentioned above, which only concentrate on one or two processes, are difficult to account for these challenges. Moreover, along with the rapid development of computer sciences and earth observation technologies in the last decade, the new generation of water system models should consider multiple processes and interactions in more detail.

The objective of this study is to develop a new hydrological and biogeochemical process-oriented water system model with the aim to predict the spatial and temporal variations of several key elements (e.g. evapotranspiration, soil water, runoff, nonpoint

HESSD
11, 9219–9279, 2014

source pollution, water quality variables in water body, crop yield and greenhouse gas emissions) in disturbed basins. The model framework is put forward based on the interchange and balancing processes of water, heat and mass which are depicted by several robust models. The parameter analysis module is also included in our programming codes.

In this paper, the model performance is illustrated by a case study in China. This study is expected to provide a new approach and reference to develop integrated water system model in highly disturbed basins, to lay the scientific foundation to promote the implement of integrated river basin management all over the world.

The paper is organized as follow. The model framework and individual modules are introduced in Sect. 2, followed by the case study, including data pre-processing, the calibration criteria, model performance. Conclusions and perspective discussions are drawn in Sect. 4.

2 Model framework

In this study, the considered water related processes in a complex basin are illustrated in Fig. 1. This model is developed along with SWAT structure with the following key differences. First, note that the Soil Conservation Service (SCS) curve number adopted in SWAT to estimate surface runoff is an empirical model developed for rural watersheds in the United States. However, the applicability of SCS curve number to other regions has been questioned (Rallison and Miller, 1981). The proposed model uses Time Variant Gain Model (TVGM) (Xia et al., 2005) to calculate surface runoff yield because of its strong theoretical basis. Second, note that SWAT describes the complicated dynamic processes of soil nitrogen by a simple conceptual approach which is weak in capturing some of these processes accurately (Gassman et al., 2007). The proposed model prefers the strongly physical based DNDC model.

The proposed model is named HE^XM where **H** indicates **H**ydrological submodel and **X** is used to indicate **E**cological, **E**nvironmental submodels with possible future extension to **E**conomic submodel (water consumption processes in the soc-economy system). There are seven major modules in HE^{X}M, named as hydrological cycle module (HCM) based on hydrology; soil biochemical module (SBM) and crop growth module (CGM) based on ecology; soil erosion module (SEM), mass migration module (MMM) and water quality module (WQM) for environment, as well as dams regulation module (DRM). Parameter analysis tool (PAT) is a useful post-processing tool for HE^{X}M calibration and is independent from other modules. The model takes full advantages of powerful interconnection and simulation functions of hydrological model at large spatial scale, elaboration of vertical movement of materials in soil layers of ecological model at site scale and longitudinal movement of materials in river segments of environmental model. The exterior exchange elements connecting different modules are given in Fig. 1. The interior elements of each module have not been listed in order to better present the model structure and the relationship of these modules. More detailed description of each module and its interactions with other modules are given in the following sections. In order to make the presentation of the paper more readable, the main equations of each process are deferred to the Appendices for readers who are interested in the mathematical details.

2.1 Hydrological cycle module

Hydrological process controls physiological and ecological processes of vegetation, oxidation-reduction reaction and anaerobic reaction of materials in soil layers, spatial and temporal distribution of water and pollutant in the basin. A flowchart is given in Fig. 2, from which it can be seen that shallow soil water from HCM is one of the major factors connecting CGM (to control crop growth) and SBM (to control vertical migration and reaction of materials in soil profiles). Plant transpiration is also linked to SBM (to provide energy for vertical migration of materials in soil profiles). The overland flow including surface runoff and soil runoff is linked to SEM and MMM (to drive longitude migration of matter and sediment along flow paths), to WQM for runoff routing in water bodies (rivers and lakes). Moreover, HCM calculates inflow of dams or sluices for DRM.

HESSD
11, 9219–9279, 2014

Surface runoff yield calculation is the core of hydrological simulation and has close relationships with many other processes. Time Variant Gain Model (TVGM) (Xia et al., 2005) is applied to calculate surface runoff yield because of its strong theoretical basis. In TVGM, the rainfall–runoff relationship is nonlinear with surface runoff coefficient varying and being affected significantly by antecedent soil moisture (Xia et al., 1991). TVGM is based on the Volterra function and has satisfactory performance, especially in arid and semiarid regions (Xia et al., 2005; Wang et al., 2009).

The potential evapotranspiration is calculated using Hargreaves method (Hargreaves and Samani, 1982) because it only uses the daily maximum and minimum temperature data which are widely available. The actual plant transpiration is expressed as a function of potential evapotranspiration and leaf area index while the soil evaporation is expressed as a function of potential evapotranspiration and surface soil residues. The soil and ground runoff is considered as a linear storage–outflow relationship (Wang et al., 2009). The infiltration from the upper to lower soil layer is calculated using storage routing methodology (Neitsch et al., 2005). The Muskingum method or kinetic wave equation is used for river flow routing.

2.2 Ecological process modules

Ecosystem is one of the decisive components to the hydrological cycle and the material migration and transportation. The main feature of HE^XM is that water cycle, nutrient cycles and crops growth, as well as their key linkages are incorporated. The ecological processes contain SBM and CGM modules.

2.2.1 Soil biochemical module (SBM)

SBM simulates the key processes of Carbon (C), Nitrogen (N) and Phosphorus (P) dynamics in the soil profiles, including decomposition, mineralization, immobilization, nitrification, denitrification and plant uptake, etc. C constrains the decomposition and denitrification of N and P. Soluble nutrient including nitrate nitrogen (NO_3-N), NH_4-

HESSD
11, 9219–9279, 2014

Integrated hydrological-biogeochemical system model

Y. Y. Zhang et al.

N and soluble P outputted from SBM are connected to CGM as nutrient constraint of crop growth, and to MMM as main sources of pollutant to water bodies as well as insoluble materials (organic P and N) (Fig. 3a). The daily step decomposition and denitrification submodels in DNDC (Li et al., 1992) are adopted to simulate biogeochemical processes of C and N in the soil profile at site scale (Li et al., 1992). The major processes of soil P cycle are simulated based on the studies of Horst et al. (2001) and Neitsch et al. (2005). The soil profile is divided into three layers, viz. surface (0–10 cm), and user defined upper and lower layer.

Soil C and N cycle. In the aerobic state, the decomposition and other oxidation processes, such as nitrification, mineralization and immobilization, are the dominant microbial processes. The denitrification process is activated by rainfall or irrigation events. As the oxygen availability is limited, a series of N oxides is used to replace oxygen as the terminal electron acceptor during soil oxidation-reduction reaction.

- *Decomposition.* There are three conceptual organic C pools: the decomposable residue pool, microbial biomass pool and a stable pool (humus). Every pool contains resistant and labile components. Decomposition of each C pool is treated as the first-order decay process with the individual decomposition being modified by soil temperature and moisture, clay content and the C : N ratio. Carbon dioxide (CO_2), released from soil organic carbon (SOC), is calculated as a constant fraction of the C undergoing decomposition of three C pools. When precipitation and/or irrigation happen, the decomposition process will pause and the denitrification process will start until the soil water file pore space (WFPS) in the surface soil layer reaches a threshold (e.g. 40 %) or the substrates are used up. Then the decomposition will restart. The details of SOC pool structure are described in Li et al. (1992).

- *Nitrogen transformation during decomposition*. The major simulated processes with decomposition under aerobic condition are mineralization, immobilization, ammonia (NH_3) volatilization and nitrification. Ammonium (NH_4^+) is mineralized

HESSD
11, 9219–9279, 2014

from organic N pool when SOC flows from lower C : N ratio C pools into higher C : N ratio C pools. During immobilization, if the mineral N (NH_4^+ and NO_3-N) is not enough, SOC decomposition will reduce to an allowable level. NH_3 volatilization is controlled by NH_4^+ concentration, clay content, pH, soil moisture and temperature. NH_4^+ is microbial oxidized to NO_3-N and nitrous oxide (N_2O) which emit into the air as a gaseous intermediate during nitrification. The proportion of N_2O is small and is controlled by NH_4^+ concentration, pH, temperature, moisture, etc in the soil layer.

– *Denitrification.* The denitrification process works during rainfall or irrigation events when WFPS is greater than the threshold. The general recognized reduction sequence in denitrification is $NO_3 \rightarrow NO_2 \rightarrow NO \rightarrow N_2O \rightarrow N_2$. The denitrification rate correlates with denitrifier biomass, moisture, pH, temperature, and NO_3-N concentration in the soil layer. The denitrifier biomass is estimated with the growth and dead rate of denitrifier which is controlled by soluble soil C and soil moisture, temperature. The C and N from dead cells are added to the pools of immobilized C and N which no longer participate in the dynamic processes. The consumption rate of soluble C depends on the biomass, relative growth rate, and the maintenance coefficients of the denitrifier populations. The daily emissions of N_2O and N_2 are calculated as a proportion of total production of N_2O and N_2 which is related to the adsorption coefficients of gases in soils and the air filled porosity of the soil. But the emission is neglected because of the low diffusion rates in soil water during the rainfall events.

Soil P cycle. Four major forms of P in soils are considered, viz., stable organic P, active organic P for plant uptake, fresh organic P associated with plant residue, microbial biomass and soluble mineral P as the consequence of mineralization, decomposition and sorption (Horst et al., 2001). The P dynamics processes are considered in Horst et al. (2001) and Neitsch et al. (2005), through modeling the P release from fertilizer,

Discussion Paper | Discussion Paper | Discussion Paper | Discussion Paper |

HESSD

11, 9219–9279, 2014

Integrated hydrological-biogeochemical system model

Y. Y. Zhang et al.

manure, residue, microbial biomass and humic substances, and plant uptake and transport by soil erosion.

2.2.2 Crop growth module (CGM)

CGM is developed based on EPIC crop growth model (Hamrick, 1992), which applies the concept of daily accumulated heat units on phonological crop development, with Monteith's approach for potential biomass, harvest index for partitioning grain yield, stress adjustments for water, temperature, and N availability in the root zone of the soil profile. It predicts total dry matter, leaf area index, root depth and density distribution, harvest index, and N uptake, etc. (Willians et al., 1989; Sharpley and Williams, 1990). The crop respiration and photosynthesis drive the vertical movement of water and nutrient, and transpiration. In CGM, the output of leaf area index is the main factor connecting HCM (to control the transpiration), and the crop residues left in the fields is the main source of organic materials (N, P and C) connecting to SBM for soil biochemical degradation, to MMM for overland migration, and to SEM as one of the five constraint factors (Fig. 3b).

2.3 Environmental process modules

The environmental process modules are to simulate the material (e.g., different forms of nutrient, chemical oxygen demand) migration and transformation with the movement of surface water and sediment. The main modules are SEM for simulating sediment yield, MMM for material migration to water bodies (rivers or lakes) with overland flow and sediment, WQM for the migration and transformation in water bodies.

2.3.1 Soil erosion module (SEM)

The soil erosion by precipitation is estimated using the improved ULSE equation (Onstad and Foster, 1975) based on runoff outputted from HCM, crop management factor outputted from CGM. SEM simulates sediment load for MMM to provide the

HESSD
11, 9219–9279, 2014

carrier for the migration of insoluble organic materials in overland and water bodies (Fig. 4a).

2.3.2 Mass migration module (MMM)

The main mass migration processes contain the soluble matter migration with overland runoff, the adsorbed matter migration with sediment, immobilization and mineralization, as well as the loss during the migration. This module calculates the matter load discharged into rivers for WQM (Fig. 4b).

2.3.3 Water quality module (WQM)

Two water quality modules are designed for different types of water bodies, viz., the in-stream water quality module and the water quality module of water impounding (reservoir or lake). The enhanced stream water quality model (QUAL-2E) (Brown and Barnwell, 1987), as a comprehensive and versatile stream model, is adopted to simulate the longitudinal movement and transformation of water quality constituents in the branch stream systems. The model is centered at dissolve oxygen (DO) and can simulate up to 15 water quality constituents including temperature, DO, sediment, different forms of nutrient (N and P), chemical oxygen demand (COD), pesticide, coliform bacteria, and three conservative constituents (Neitsch et al., 2002) (Fig. 4c). The mass balance is used to determine the constituents' concentration based on the mass fluxes into and out of each computational unit and the degradation of the constituents themselves. The water quality outputs are linked to DRM to provide upper water quality boundary of dams or sluices. The water quality module of water impounding assumes that water body is at the steady state and focuses on the vertical interaction of constituents. The main processes are the constituent's degradation, settlement, resuspension and decay in the sediment.

HESSD
11, 9219–9279, 2014

2.4 Dams regulation module (DRM)

The dams or sluices highly disturb the flow regimes and associated eco-environmental processes in most river networks (Zhang et al., 2013). The regulation of dams or sluices should be considered in water system models. DRM provides hydrological boundaries (e.g. water storage, runoff) regulated by dams or sluices to HCM for flow routing and to WQM for matter migration (Fig. 5).

In our system, four methods are proposed for calculating water storage and outflow of dams or sluices, viz.: no regulation, measured daily or monthly outflow, controlled outflow with target water storage, and the relationship between outflow and water storage volume (Neitsch et al., 2002; Zhang et al., 2013). The no regulation method ignores the regulation rules and does not need any data. The measured daily or monthly methods require users to provide the measured daily or monthly outflow series during the simulation period. The third method simplifies the regulation rule of dam or sluice for the long-term analysis, that is, it assumes that water is stored according to the usable water level during the non-flooding season and the flood control level during the flooding season and that the redundant water is discharged. The method requires the characteristic parameters of dam or sluice including water storage capacities of dead, usable, flood control and maximum flood levels and the corresponding water surface areas. The fourth method is proposed according to the actual situation of China (Zhang et al., 2013).

2.5 Parameter analysis tool (PAT)

Parameter sensitivity analysis and auto-calibration are critical steps for the applications of highly parameterized models, especially the integrated water system models (McDonnell et al., 2007). Several parameter analysis methods are coupled in HE^{X}M, including parameter sensitivity method (Latin Hypercube One factor At a Time: LH-OAT) (van Griensven et al., 2006), auto-optimization methods such as Particle Swarm Optimization (PSO) (Kennedy, 1995), Genetic Algorithm (GA) (Goldberg, 1989) and

HESSD
11, 9219–9279, 2014

Shuffled Complex Evolution (SCE-UA) (Duan et al., 1994) as well as uncertainty analysis method (Bayesian approach).

2.6 Datasets and spatial delineation

The indispensable spatial and temporal datasets of HE^{X}M are GIS data (DEM, soil physical and chemical properties, land use and crop types), daily meteorological data (precipitation, maximum and minimum air temperature), social-economic data (populations in urban and rural area, total gross domestic product: GDP and secondary industry GDP, orchard area, breeding stock of large animals and livestock, chemical fertilizer amount and cultivation methods, water withdrawal and point source pollutant load), dams characteristic data (water storage capacities of dead, usable, flood control and maximum flood levels and the corresponding water surface areas). Several monitoring data series are also needed to calibrate HE^{X}M such as runoff or water quality series at river sections, soil water content and crop yield at the field scale. All the datasets and their usages in HE^{X}M are given in Table 2.

The model is setup based on sub-basins at daily scale. The hydrological toolset of Arc GIS 10.0 platform, or AVSWAT platform are used to delineate sub-basins, river system and flow routing relationship between sub-basins based on DEM. Generally, the minimum simulation cells are partitioned in each sub-basin related to the main landuse classes of the classification standard of China including forest, grassland, water, urban, unused land, paddy land and dry land (GB/T21010-2007).

Different modules are linked as following. The overland yield and reaction processes of water, material and crop of HE^{X}M are simulated in the minimum simulation cell of each sub-basin and related modules include HCM (e.g., water yield, inflitration, interception and evapotranspiration), SBM, SEM and CGM. The migration processes of water and material are calculated in each sub-basin and its related modules is HCM (e.g., flow routing), MMM, WQM and DRM.

HESSD
11, 9219–9279, 2014

3 Model application and results

As an example, HE^{X}M is applied in a highly regulated and heavily polluted river basin of China in order to test the model performance. The simulated components contain daily runoff and water quality concentration at several river cross-sections, spatial patterns of nonpoint source pollutant load and crop yield at sub-basin scale. Furthermore, the simulation results are compared with the existing studies calculated by another widely-used model (SWAT) in the same area (see Zhang et al., 2013).

3.1 Study area

Shaying River Catchment (112°45′ ~ 113°15′ E, 34°20′ ~ 34°34′ N), as the largest sub-basin of Huai River Basin in China, is selected as our study area (Fig. 6a). It has the drainage area of 36 651 km^2 and the mainstream of 620 km long. The basin is located in the typical warm temperate, semi-humid continental climate zone. The annual average temperature and rainfall are 14–16 °C and 769.5 mm, respectively. Meanwhile, Shaying River is the most serious polluted tributary with pollutant load contributing over 40 % of the whole Huai River and is usually known as the water environment barometer of Huai River mainstream. In order to reduce flood or drought disasters, 24 reservoirs and 13 sluices have been constructed and fragment river into several impounding pools which control over 50 % of the total annual runoff.

3.2 Model setup and evaluation

Shaying River Catchment is then divided into 46 sub-basins and the land use types are dry land (84.04 %), forest (7.66 %), urban (3.27 %), grassland (2.68 %), water (1.43 %), paddy (0.91 %) and unused land (0.01 %) (Fig. 6b). The soil input parameters (the contents of sand, clay and organic matter) are calculated based on the percent of soil types in each sub-basin.

HESSD
11, 9219–9279, 2014

The daily data series at 65 precipitation stations and six temperature stations are interpolated to each sub-basin from 2003 to 2008, using the inverse distance weighting method and the nearest-neighbor interpolation method, respectively. The social-economic data are also interpolated into each sub-basin based on the area percentage. There are 23 major dams and sluices and over 200 pollutant outlets considered in the model according to the geographical positions.

LH-OAT is used to test the sensitive parameters in HE^XM. The model calibration is conducted step-by-step using SCE-UA as follow. Hydrological parameters are calibrated firstly according to observed runoff series at each station from upstream to downstream, and then water quality parameters according to observed NH_4-N concentration series. The calibration and validation periods are from 2003 to 2005 and from 2006 to 2008, respectively. Bias (bias), correlation coefficient (r) and coefficient of efficiency (NS) are used to evaluate model performance.

$$\text{Bias(bias)}: \ \text{bias} = \sum (O_i - S_i) / \sum O_i \tag{1}$$

$$\text{Correlation coefficient}: \ r = \sum (O_i - \overline{O}) \cdot (S_i - \overline{S}) \Big/ \sqrt{\sum (O_i - \overline{O})^2 \cdot \sum (S_i - \overline{S})^2} \tag{2}$$

$$\text{Coefficient of efficiency}: \ \text{NS} = 1 - \sum (O_i - S_i)^2 / \sum (O_i - \overline{O})^2 \tag{3}$$

Here, O and $\overline{O}$ are the observed value and its average value, respectively; S and $\overline{S}$ are the simulated value and its average value, respectively; bias measures the average deviation between the simulated and observed counterparts whose optimal statistical value is close to 0. The optimal statistical values of r and NS are close to 1. NS is usually used to evaluate the simulation of continuous time series. However, as there are only two or three observed values of NH_4-N concentration in each month, NS is not used to evaluate the NH_4-N concentration simulation. In the model calibration, a weighted average method is used to aggregate these three objective functions to a single objective (f_{runoff} and $f_{NH_4\text{-}N}$) and the optimal statistical values are also close to

HESSD
11, 9219–9279, 2014

0 (Madsen, 2003; Efstratiadis and Koutsoyiannis, 2010).

$$\begin{cases} f_{\text{runoff}} = \min[(|\text{bias}| + 2 - r - \text{NS})/3] \\ f_{\text{NH}_4-\text{N}} = \min[(|\text{bias}| + 1 - r)/2] \end{cases} \tag{4}$$

3.3 Parameter sensitivity analysis

Over 200 parameters control the hydrological, ecological and environmental processes of HE^XM. All these parameters are categorized into 93 lumped parameters for the whole basin and 112 distributed parameters for each sub-basin according to the degree of spatial heterogeneity. It is very time-consuming and impractical to calibrate all these parameters. Thus LH-OAT is used to determine the sensitive parameters.

Nine most sensitive parameters are detected for runoff simulation (Table 3) including soil related parameters WMc, WM, k_r and f_c; TVGM parameters g_1 and g_2 for surface water calculation; ground water recharge parameters k_g and T_g; and adjusted factor KET_p of evapotranspiration. All of these parameters control the main hydrological processes, in which soil water and evapotranspiration processes are distinctly important, explaining 54.3 and 23.2 % of the runoff variation, respectively.

For NH_4-N concentration simulation, over 90 % of observed NH_4-N concentration variation are explained by 14 sensitive parameters which are categorized into hydrological (59.28 % of variation), NH_4-N (20.65 % of variation) and COD (12.34 % of variation) related parameters (Table 3). Hydrological processes provide the hydrological boundaries which affect the nonpoint source pollutant load into rivers, the degradation and settlement processes of NH_4-N in water bodies (rivers and reservoirs) (van Griensven et al., 2002). NH_4-N concentration is further influenced by the settling and biological oxidation processes. Moreover, it is a competitive relationship between COD and NH_4-N to consume DO of water bodies in a certain limited level (Brown and Barnwell, 1987).

HESSD
11, 9219–9279, 2014

3.4 Hydrological simulation

The daily runoff hydrographs are reproduced at seven regulated stations and one less-regulated station (viz., the upperstream stations unaffected by dams, or downstream stations situated far from dams). The simulations are well fitted with the observations at all the stations from the midstream to downstream (Fig. 7 and Table 4). The bias at all the regulated stations are very close to 0.0 except the underestimation at Zhoukou (0.24 for calibration and 0.41 for validation), and the overestimation at Mawan (−0.44) and Luohe (−0.52) during the validation period. The r values range from 0.61 (Huangqiao for validation) to 0.92 (Yingshang for calibration) with the average value of 0.81 while the NS values range from 0.23 (Huangqiao for validation) to 0.84 (Yingshang for calibration) with the average value of 0.63. The predictions at the regulated stations are little worse than that at the less-regulated stations due to the regulations.

Improved SWAT 2000 was also well calibrated to simulate the long-term runoff in the same area (Zhang et al., 2013). Only monthly runoff was simulated because it is difficult to forecast accurately the regulated daily runoff processes. The f_{runoff} values by SWAT at monthly scale range from 0.08 (Luohe for calibration) to 0.61 (Shenqiu for validation) (Table 4). However, our model captures the daily runoff processes very well at most stations, particularly for high flow regimes. Compared with the results of Zhang et al. (2013), the f_{runoff} calculated at the monthly scale is significantly improved for both calibration and validation at most of the downstream stations including Huangqiao, Huaidian, Fuyang, Yingshang and Shenqiu although it become little worse at the upstream stations, viz., from 0.08 to 0.14 at Luohe and from 0.12 to 0.19 at Zhoukou for calibration, from 0.19 to 0.24 for calibration and from 0.30 to 0.38 for validation at Mawan.

Because of the high regulation in most rivers, it is necessary to consider the impact of dam's regulation in the integrated water system models. All the dams and sluices are designed to control floods and supply water (Zhang et al., 2013). Thus the discharge is usually decrease and high flow events are flattened by storage.

HESSD
11, 9219–9279, 2014

The high and low flow is determined by flow duration curves and the threshold is 50 % for easy presentation. That is, the flow is high flow if its percentile is greater than the threshold, whereas it is low flow. Compared the simulated high and low flow with the observations from 2003 to 2008, flows are usually overestimated at all the stations without considering the regulations and the scatters between simulated regulated hydrographs and observations tend to more closely to the 1 : 1 line for both low and high flow events. Except the high flow simulation at Huangqiao and Zhoukou, all the high and low flow events at all the stations are better simulated with the consideration of dams and sluices regulation (Fig. 8 and Table 5). The best fitting is at Fuyang, especially for the high flow simulation (bias = 0.10, r = 0.89 and NS = 0.78). The improvements of f_{runoff} from unregulation to regulation settings range from −0.09 (Fuyang) to −0.20 (Huaidian) for high flow simulation except Huangqiao and Zhoukou (0.01), from −0.06 (Zhoukou) and −0.34 (Mawan) for average flow simulation, and from −3.16 (Huangqiao) and −15.28 (Luohe) for low flow simulation. The low flow simulation still need to be further improved as low flow forecasting is actually a difficult task and the common evaluation criteria are disadvantageous to evaluate low flow simulation (Pushpalatha et al., 2012).

3.5 Environmental simulation

NH_4-N concentration is one of the widely used indexes to assess water environmental quality in China (CSEPA, 2002). The observation series at five regulated stations and two less-regulated stations in the middle and downstream are used to calibrate the related parameters of environmental processes. The spatial distribution of nonpoint source pollutant load is also estimated.

The simulated concentrations show good agreements with the observations (Fig. 9 and Table 6). The r values of all the stations are over 0.60 expect Zhoukou (0.56 for validation), Yingshang (0.49 for validation) and Shenqiu (0.41 for validation) with the average value of 0.66. The bias of all the stations are considered as "acceptable" with the range from −0.27 (Fuyang for validation) to 0.29 (Zhoukou for calibration)

HESSD
11, 9219–9279, 2014

except Fantaizi (0.45 for calibration and −0.62 for validation). The best simulation is at Luohe. As the accuracy of water quality simulation is directly influenced by hydrological simulation (Zhang et al., 2013), the unacceptable bias at Fantaizi might be attributed by the uncertainties existed in the uncalibrated hydrological processes. Moreover, the underestimated concentrations often emerge in the period from January to May due to the overestimation of low flows.

Compared with the results of Zhang et al. (2013), all the values of $f_{NH_4\text{-}N}$ decrease obviously with the range from −0.02 (Fantaizi for validation) to −0.61 (Fuyang for validation) except Zhoukou (0.16 for calibration). The NH_4-N simulation performance of HE^XM has been improved greatly by coupling process-based N cycle model (DNDC), but little weaker at Zhoukou during the calibration period due to the runoff simulation error. The simulation is also significantly improved considering the regulation compared to the results without the regulation except Fuyang for calibration. The decreases of $f_{NH_4\text{-}N}$ value range from 0.06 (Fantaizi for calibration) to 0.49 (Zhoukou for validation). The degradation and settlement at the upstream of dams or sluices play a positive role in pollutant concentration reduction by water storage. Thus, the simulated concentrations without regulation are greater than the observation or the simulation with regulation, except Huaidian, and the largest difference appears at Zhoukou.

The spatial pattern of average annual nonpoint source NH_4-N load is shown in Fig. 10. The modeled annual yield rates range from 0.048 to 11.00 with a mean of $0.73\,t\,km^{-2}\,year^{-1}$. The high load yield regions are in the middle of Pingdingshan, Xuchang, Zhengzhou, Fuyang and Zhoukou cities. The spatial pattern is highly correlated with the distribution of paddy fields ($r = 0.506$) and the rice yield ($r = 0.799$). The fertilizer loss of paddy fields is the primary contributor to the nonpoint source NH_4-N load, possibly because the average nitrogen use efficiency in China is just 30 ∼ 70 % in paddy fields, which is much lower than the efficiency in the dry field (50 ∼ 80 %). The nitrogen is easy to loss by volatilization to air, dissolution and drainage into rivers with runoff in paddy fields (Gao et al., 2008).

HESSD
11, 9219–9279, 2014

Furthermore, the average annual point source NH_4-N loads into rivers are about 4.70×10^4 t year^{-1} in Shaying River Catchment by statistics. Thus, nonpoint source load contributes 38.57 % of the overall NH_4-N load on average from 2003 to 2005, which is little greater than the statistics results (29.37 %) of integrated water resources planning of Huai River Basin and Shandong Peninsula in 2000. Compared with the nonpoint source load of each city in 2000, the simulated annual loads tend to increase from 2003 to 2005 except in Kaifeng city. The most increased regions are Fuyang and Pingdingshan cities.

3.6 Crop yield simulation

The simulated corn yield and its spatial pattern are shown in Fig. 11. The average annual yields range from 28.10 to 762 169.64 with the mean of 63 704.40 t year^{-1}. The high-yield regions are Fuyang and Zhoukou cities in the middle and down reaches, whose primary land use are dry land (95.87 and 93.18 %, respectively). According to the statistics at city scale, the yields of Luohe, Nanyang, Kaifeng cities are well simulated compared with the statistics from statistical yearbooks from 2003 to 2005 (Henan Statistical Yearbook, 2003, 2004 and 2005). The total yield is underestimated in the whole basin with the relative error of 19.93 %. The boundary mismatch between cities and sub-basins results in the simulated errors, as well as the different cropping patterns in such huge basin. Higher resolution remote sensing image and field investigation can further improve the model performance.

4 Conclusions

Integrated river basin management is facing severe complicated water issues caused by the high interference of human activities and climate change. It is difficult to solve these water problems by the traditional hydrological method because of the high interconnections in the complicated water system. Water system modeling is

HESSD
11, 9219–9279, 2014

an effective approach for integrated water governance in the complex basins. It provides a new research direction and is a hot-topic in water related sciences. In this study, a process-oriented water system model (HE^{X}M) was developed and applied in the Shaying River, China. Several key elements of major processes were modeled including runoff, water quality concentrations, nonpoint source pollutant load and crop yield. The results showed that:

1. Hydrological cycle was strongly associated with biogeochemistry, ecological processes, as well as climate change and highly intensive human activities. However, most of the existing models focused on individual or two processes at the site or basin scale, which were disadvantageous to solve the present water-related problems. For examples, the traditional hydrological models paid attention to flood forecast or water resources assessment at the basin scale. In-stream water quality models focused on the migration and transformation of pollutants in water bodies. The mature ecological models and biogeochemical models concerned the nutrient and water cycles and physiological and ecological processes of vegetations at the field or experimental catchment scale. HE^{X}M was a science-based approach to integrate and simulate multi-scale processes of hydrology, biogeochemistry, crop physiology and growth, environment, as well as their interactions based on the classical single mathematics models. The proposed model could estimate the major hydrological elements (viz., soil water and evaporation, plant transpiration, runoff and water storage in the dams and sluices), environmental elements (viz., nonpoint source pollutant load, different forms of N / P / C, water quality indexes in water bodies), ecological elements (leaf area index, crop yield and greenhouse gas emission) in the complex basins.

2. Integrated water system management should obey the principle that both human activities and water-related systems are in naturally functioning condition, and coordinate the planning, development, management and use of land, water and related natural resources within hydrological boundaries (Watson, 2004).

Thus, the variation of several indicative elements of each subsystem should be provided in real-time to support the integrated regulation and management. Process-oriented water system model could play a critical technical role in the implementation of integrated management. HE^XM was a successful practice and could be a reference point for integrated complex water system management in the highly disturbed basins.

3. In the case study, the simulated daily runoff at all the stations was well fitted with the observations. All the evaluation criteria were acceptable except at one or two stations. Moreover, HE^XM well captured the variation of discontinuous daily NH_4-N concentration and the unacceptable bias at some stations might be attributed by the uncertainties existed in the uncalibrated hydrological processes. The spatial patterns of nonpoint source pollutant load and corn yield were also properly simulated. The outputs of several cities were good agreements with the statistics. The model performances were significantly improved in comparison with the existing model results. HE^XM can better simulate runoff and water quality concentration at the daily scale in the highly regulated basins, especially for the high and low flow events. The objective function values of both runoff and NH_4-N simulation were much greater than that by the improved SWAT simulation (Zhang et al., 2013) and the results without considering regulation.

Restricted by the heterogeneity of spatial data in large basins and insufficient observations of every subsystems, not all the results were acceptable and several critical processes were not well calibrated (low flow regimes, greenhouse gas emission, crop yield, soil erosion and nonpoint source pollutant load, etc.). The model structure could be further developed and calibrated with the absorption of new observation sources. More complex humanity activities and water-related processes in economy system will be incorporated into this model once the interaction mechanisms with natural hydrologic cycle could be depicted accurately. Furthermore, there are still several great challenges in combined calibration of multi-component and model

HESSD
11, 9219–9279, 2014

uncertainty analysis because of the interaction among different processes and highly parameterization (Beven and Binley, 1992; Grayson et al., 1992). Advanced mathematic analysis technologies should be applied to in the next works (Gupta et al., 1998; Reichert and Schuwirth, 2012).

Appendix A: Hydrological cycle modules

The basic water balance equation is

$$P_i + \mathrm{SW}_i = \mathrm{SW}_{i+1} + \mathrm{Rs}_i + E_{\mathrm{ai}} + \mathrm{Rss}_i + \mathrm{Rg}_i + \mathrm{In}_i \tag{A1}$$

where P is precipitation (mm); SW is soil water moisture (mm); E_{ai} is actual evapotranspiration including soil evaporation and plant transpiration (mm); Rs, Rss and Rg is surface runoff, soil runoff and ground runoff (mm), respectively; In is the vegetation interception (mm) and i is the time step (days).

The actual soil evaporation (E_s) and plant transpiration (E_p) is determined by potential evapotranspiration (E_0), leaf area index (LAI) and surface soil residues (rsd) (Ritchie, 1972), viz.,

$$\begin{cases} E_\mathrm{a} = E_\mathrm{p} + E_\mathrm{s} \le E_0 \\ E_\mathrm{p} = f(\mathrm{LAI}) \cdot E_0 \\ E_\mathrm{s} = f(\mathrm{rsd}) \cdot E_0 \end{cases} \tag{A2}$$

where $f(\cdot)$ is a linear or nonlinear function. E_0 is calculated by Hargreaves method.

The surface runoff yield equation (TVGM; Xia et al., 2005) is as following.

$$\mathrm{Rs} = g_1 (\mathrm{SW_u}/W_{\mathrm{sat}})^{g_2} \cdot (P - \mathrm{In}) \tag{A3}$$

where $\mathrm{SW_u}$ and W_{sat} are surface soil moisture and saturation moisture (mm), respectively; g_1 and g_2 are coefficient of basic runoff and soil moisture, respectively.

HESSD
11, 9219–9279, 2014
Integrated hydrological-biogeochemical system model
Y. Y. Zhang et al.

The soil and ground water flow are considered as a linear storage–outflow relationship (Wang et al., 2009).

$$\begin{cases} \mathrm{Rss} = k_\mathrm{r} \cdot \mathrm{SW_u} \\ \mathrm{Rg} = k_\mathrm{g} \cdot \mathrm{SW_l} \end{cases} \tag{A4}$$

where k_r and k_g are soil and ground water flow yield coefficient. $\mathrm{SW_l}$ is soil moisture of lower layer (mm).

The infiltration from the upper to lower soil layer is calculated using storage routing methodology (Neitsch et al., 2005), viz.,

$$\begin{cases} W_\mathrm{inf} = (\mathrm{SW_u} - W_\mathrm{fc}) \cdot (1 - \exp(-t/T_\mathrm{inf})) \\ T_\mathrm{inf} = (W_\mathrm{sat} - W_\mathrm{fc})/K_\mathrm{sat} \end{cases} \tag{A5}$$

where W_inf is water infiltration amount on a given day (mm); W_fc is soil field capacity (mm); t and T_inf are time step and travel time for infiltration (h), respectively; and K_sat is saturated hydraulic conductivity (mm h^{-1}).

The overland flow routing is calculated:

$$Q_\mathrm{overl} = (Q'_\mathrm{overl} + Q_{\mathrm{stor},i-1}) \cdot [1 - \exp(-1/T_\mathrm{overl})] \tag{A6}$$

where Q_overl is overland flow discharged into main channel (mm), Q'_overl is lateral flow amount generated in the sub-basin (mm), $Q_{\mathrm{stor},i-1}$ is lateral flow lagged from the previous day (mm) and T_overl is lateral flow travel time (days).

HESSD
11, 9219–9279, 2014
Integrated hydrological-biogeochemical system model
Y. Y. Zhang et al.

Appendix B: Ecological process modules

B1 Soil biochemical module (SBM)

B1.1 Soil temperature

$$T(Z,t) = \overline{T} + (\mathrm{AM}/2 \cdot \cos[2\pi \cdot (t-200)/365] + \mathrm{TG} - T(0,t)) \cdot e^{-Z/\mathrm{DD}} \tag{B1}$$

where Z is soil depth (mm); t is time step (days); $\overline{T}$ and TG are average annual temperature and surface temperature, respectively (°C); AM is annual variation amplitude of daily temperature; DD is damping depth of soil temperature (mm).

$$\begin{cases} \mathrm{DD} = \mathrm{DP} \cdot \exp\{\ln(500/\mathrm{DP}) \cdot [(1-\xi)/(1+\xi)]^2\} \\ \mathrm{DP} = 1000 + 2500\mathrm{BD}/[\mathrm{BD} + 686\exp(-5.63\mathrm{BD})] \\ \xi = \mathrm{SW}/[(0.356 - 0.144\mathrm{BD}) \cdot Z_\mathrm{M}] \\ \mathrm{TG}_\mathrm{IDA} = (1-\mathrm{AB}) \cdot (T_\mathrm{mx} + T_\mathrm{mn})/2 \cdot (1 - \mathrm{RA}/800) + T_\mathrm{mx} \cdot \mathrm{RA}/800 + \mathrm{AB} \cdot \mathrm{TG}_{\mathrm{IDA}-1} \end{cases} \tag{B2}$$

where DP is maximum damping depth of soil temperature (mm); BD is soil bulk density ($\mathrm{t\,m^{-3}}$); ξ is scale parameter; IDA is day of the year; AB is surface albedo; RA is daily solar radiation (ly).

B1.2 C and N cycle

Decomposition. The decomposition of resistant and labile C using the first order kinetic equation, viz.

$$\mathrm{d}C/\mathrm{d}t = \mu_\mathrm{CLAY} \cdot \mu_\mathrm{C:N} \cdot \mu_\mathrm{t,\,n} \cdot (S \cdot k_1 + (1-S) \cdot k_2) \tag{B3}$$

where μ_CLAY, $\mu_\mathrm{C:N}$ and $\mu_\mathrm{t,\,n}$ is the reduction factor of clay content, C : N ratio and temperature for nitrification, respectively; S is labile fraction of organic C compounds;

k_1 and k_2 is specific decomposition rate of labile faction and resistant fraction, respectively (days^{-1}).

The ammonia amount absorbed by clay and organic materials (FIX_{NH_4}) is estimated using the equation.

$$FIX_{NH_4} = [0.41 - 0.47 \cdot \log(NH_4)] \cdot (CLAY/CLAY_{max}) \quad (B4)$$

where NH_4 is NH_4^+ concentration in the soil liquid (g kg^{-1}). CLAY and $CLAY_{max}$ are clay content and the maximum clay content, repectively.

$$\begin{cases} \log(K_{NH_4}/K_{H_2O}) = \log(NH_{4m}/NH_{3m}) + pH \\ NH_{3m} = 10^{\{\log(NH_4) - (\log(K_{NH_4}) - \log(K_{H_2O})) + pH\} \cdot (CLAY/CLAY_{max})} \\ AM = 2 \cdot (NH_3) \cdot (D \cdot t/3.14)^{0.5} \end{cases} \quad (B5)$$

where K_{NH_4} and K_{H_2O} are dissociation constant for $NH_4^+ : NH_3$ equilibrium, $H^+ : OH^-$ equilibrium, respectively; NH_{4m} and NH_{3m} are NH_4^+ and NH_3 concentration in the liquid phase, respectively (mol L^{-1}); AM and D are accumulated NH_3 loss (mol cm^{-2}) and diffusion coefficient (cm^2 d^{-2}), respectively.

The nitrification rate (dNNO kg ha^{-1} day^{-1}) is a function of the available NH_4^+, soil temperature and soil moisture. N_2O emission is a function of soil temperature and soil NH_4^+ concentration, viz:

$$\begin{cases} dNNO = NH_4(t) \cdot [1 - \exp(-K_{35} \cdot \mu_{t,n} \cdot dt)] \cdot \mu_{m,n} \\ N_2O = (0.0014 \cdot NH_4/30.0) \cdot (0.54 + 0.51 \cdot T)/15.8 \end{cases} \quad (B6)$$

where NH_4(t) is available NH_4^+ (kg ha^{-1}); K_{35} is nitrification rate at 35 °C (mg kg ha^{-1}); $\mu_{m,n}$ is moisture adjusted factor for nitrification.

HESSD
11, 9219–9279, 2014
Integrated hydrological-biogeochemical system model
Y. Y. Zhang et al.

Denitrification. The growth rate of denitrifier is proportional to their respective biomass, which is calculated with double Monod kinetics equation.

$$\left\{\begin{array}{l}(\mathrm{d}B/\mathrm{d}t)_\mathrm{g} = \mu_\mathrm{DN}\cdot B(t)\\ \mu_\mathrm{DN} = \mu_\mathrm{t,\,dn}\cdot(u_{\mathrm{NO_3}}\cdot\mu_{\mathrm{PHNO_3}} + u_{\mathrm{NO_2}}\cdot\mu_{\mathrm{PHNO_2}} + u_{\mathrm{N_2O}}\cdot\mu_{\mathrm{PHN_2O}})\\ u_{\mathrm{N_xO_y}} = u_{\mathrm{N_xO_y,max}}\cdot(\mathrm{C}/K_{\mathrm{C},1/2}+\mathrm{C})\cdot(\mathrm{N_xO_y}/K_{\mathrm{N_xO_y},1/2}+\mathrm{N_xO_y})\end{array}\right. \tag{B7}$$

where B is denitrifier biomass (kg); $(\mathrm{d}B/\mathrm{d}t)_\mathrm{g}$ is potential growth rate of denitrifier biomass ($\mathrm{kg\,ha^{-1}\,day^{-1}}$); μ_DN is relative growth rate of the denitrifiers; $u_{\mathrm{N_xO_y}}$ and $u_{\mathrm{N_xO_y,max}}$ are relative and maximum growth rate of NO_2^-, NO_3^- and N_2O. $\mu_{\mathrm{PHN_xO_y}}$ and $\mu_\mathrm{t,\,dn}$ are reduction factor of soil pH and temperature, respectively.

$$\left\{\begin{array}{l}\mu_{\mathrm{PHNO_3}} = 7.14\cdot(\mathrm{pH}-3.8)/22.8\\ \mu_{\mathrm{PHNO_2}} = 1.0\\ \mu_{\mathrm{PHN_2O}} = 7.22\cdot(\mathrm{pH}-4.4)/18.8\\ \mu_\mathrm{t,\,dn} = \begin{cases}2^{(T-22.5)/10} & \text{if } T < 60\,^\circ\mathrm{C}\\ 0 & \text{if } T \geq 60\,^\circ\mathrm{C}\end{cases}\end{array}\right. \tag{B8}$$

The death rate of denitrifier $(\mathrm{d}B/\mathrm{d}t)_\mathrm{d}$ ($\mathrm{kg\,ha^{-1}\,h^{-1}}$) is the proportional to denitrifier biomass, viz.

$$(\mathrm{d}B/\mathrm{d}t)_\mathrm{d} = M_\mathrm{C}\cdot Y_\mathrm{C}\cdot B(t) \tag{B9}$$

where M_C and Y_C are maintenance coefficient of C ($1\,\mathrm{h^{-1}}$), maximum growth yield of soluble C, respectively.

The consumption rate of soluble C and CO_2 production is calculated as

$$\left\{\begin{array}{l}\mathrm{dC_{con}}/\mathrm{d}t = (\mu_\mathrm{DN}/Y_\mathrm{C}+M_\mathrm{C})\cdot B(t)\\ \mathrm{dCO_2}/\mathrm{d}t = \mathrm{dC_{con,\,t}}/\mathrm{d}t-(\mathrm{d}B/\mathrm{d}t)_\mathrm{d}\end{array}\right. \tag{B10}$$

HESSD

11, 9219–9279, 2014

Integrated hydrological-biogeochemical system model

Y. Y. Zhang et al.

The NO_3^-, NO_2^- and N_2O consumption are calculated with Pirt's equation.

$$\mathrm{dN_xO_y}/\mathrm{d}t = (u_{\mathrm{N_xO_y}}/Y_{\mathrm{N_xO_y}} + M_{\mathrm{N_xO_y}} \cdot \mathrm{N_xO_y}/\mathrm{N}) \cdot B(t) \cdot \mu_{\mathrm{PHN_xO_y}} \cdot \mu_{\mathrm{t,dn}} \quad \text{(B11)}$$

N assimilation is calculated on the basis of the growth rates of denitrifiers and the C : N ratio ($\mathrm{CNR_{D:N}}$) in the bacteria, viz.

$$(\mathrm{d}N/\mathrm{d}t)_{\mathrm{ass}} = (\mathrm{d}B/\mathrm{d}t)_{\mathrm{g}} \cdot (1/\mathrm{CNR_{D:N}}) \quad \text{(B12)}$$

The emission rate is a function of adsorption coefficients of the gases in soils and to the air filled porosity of the soil.

$$\begin{cases} P(\mathrm{N_2}) = 0.017 + (0.025 - 0.0013 \cdot \mathrm{AD}) \cdot \mathrm{PA} \\ P(\mathrm{N_2O}) = [30.0 \cdot (0.0006 + 0.0013 \cdot \mathrm{AD}) + (0.013 - 0.005 \cdot \mathrm{AD})] \cdot \mathrm{PA} \\ P(\mathrm{NO}) = 0.5 \cdot [(0.0006 + 0.0013 \cdot \mathrm{AD}) + (0.013 - 0.005 \cdot \mathrm{AD}) \cdot \mathrm{PA}] \end{cases} \quad \text{(B13)}$$

where $P(N_2)$, $P(NO)$ and $P(N_2O)$ are emission rate of N_2, NO, N_2O during a day, respectively; PA and AD are air-filled fraction of the total porosity and adsorption factor depending on clay content in the soil, respectively.

B1.3 P cycle (Neitsch, et al., 2002)

Mineralization. The mineralized P is added to solution P pool. The amount of active and stable organic P is calculated as

$$\begin{cases} \mathrm{orgP_{act}} = \mathrm{orgP_{hum}} \cdot \mathrm{orgN_{act}}/(\mathrm{orgN_{act}} + \mathrm{orgN_{sta}}) \\ \mathrm{orgP_{sta}} = \mathrm{orgP_{hum}} \cdot \mathrm{orgN_{sta}}/(\mathrm{orgN_{act}} + \mathrm{orgN_{sta}}) \end{cases} \quad \text{(B14)}$$

where $\mathrm{orgP_{act}}$ and $\mathrm{orgP_{sta}}$ are the amount of P in active organic pool and stable organic pool, respectively ($\mathrm{kg\,ha^{-1}}$); $\mathrm{orgP_{hum}}$ is the humic organic P in the layer ($\mathrm{kg\,ha^{-1}}$);

HESSD
11, 9219–9279, 2014
Integrated hydrological-biogeochemical system model
Y. Y. Zhang et al.

Title Page
Abstract Introduction
Conclusions References
Tables Figures
◀◀ ▶▶
◀ ▶
Back Close
Full Screen / Esc
Printer-friendly Version
Interactive Discussion

$orgN_{act}$ and $orgN_{sta}$ are the amount of N in active organic pool and stable organic pool, respectively ($kg\,ha^{-1}$).

The mineralized rate of humus active organic P pool (RHP) is calculated

$$RHP = 1.4 \cdot \beta_{min} \cdot (\gamma_{tmp} \cdot \gamma_{SW})^{1/2} \tag{B15}$$

where β_{min} is the rate coefficient for mineralization of humus active organic nutrients; γ_{tmp} and γ_{SW} are temperature factor and soil water factor.

The mineralized of the residue fresh organic P pool (RRP) is calculated as

$$\begin{cases} RRP = 0.8 \cdot \delta_{ntr} \\ \delta_{ntr} = \beta_{rsd} \cdot \gamma_{ntr} \cdot (\gamma_{tmp} \cdot \gamma_{SW})^{1/2} \end{cases} \tag{B16}$$

where δ_{ntr} and β_{rsd} are the residue decay rate and the mineralization coefficient of residue fresh organic nutrients. γ_{ntr} is the nutrient cycling residue composition factor.

Decomposition. The decomposition rate of the residue fresh organic P pool (DRP) is

$$DRP = 0.2 \cdot \delta_{ntr} \tag{B17}$$

Sorption. The P movement between soluble and active mineral pools ($P_{sol|act}$) and between active and stable mineral pools ($P_{act|sta}$) are

$$P_{sol|act} = \begin{cases} P_{sol} - \min P_{act} \cdot pai/(1-pai) & \text{if } P_{sol} > \min P_{act} \cdot pai/(1-pai) \\ 0.1 \cdot [P_{sol} - \min P_{act} \cdot pai/(1-pai)] & \text{if } P_{sol} < \min P_{act} \cdot pai/(1-pai) \end{cases} \tag{B18}$$

$$P_{act|sta} = \begin{cases} 0.0006 \cdot (4 \cdot \min P_{act} - \min P_{sta}) & \text{if } \min P_{sta} < 4 \cdot \min P_{act} \\ 0.00006 \cdot \beta_{eqP} \cdot (4 \cdot \min P_{act} - \min P_{sta}) & \text{if } \min P_{sta} > 4 \cdot \min P_{act} \end{cases} \tag{B19}$$

where P_{sol}, $minP_{act}$ and $minP_{sta}$ are soluble, mineral active and stable P, respectively ($kg\,ha^{-1}$); pai is P availability index.

Discussion Paper | Discussion Paper | Discussion Paper | Discussion Paper |
HESSD
11, 9219–9279, 2014

B2 Crop growth module (CGM)

B2.1 Crop yield

The crop growth process depends on the accumulation of daily heat (Sharpley and Williams, 1990). The accumulated heat (HU) during a day and heat unit index (HUI) is calculated as:

$$\begin{cases} \mathrm{HU}_K = (T_{\mathrm{mx},K} + T_{\mathrm{mn},K})/2 - T_{\mathrm{b},j} \\ \mathrm{HUI}_i = \sum_{K=1}^{i} \mathrm{HU}_K \Big/ \mathrm{PHU}_j \end{cases} \tag{B20}$$

where T_{mx} and T_{mn} are maximum and minimum daily temperature (°C), respectively; T_{b} is the base temperature of a certain crop (°C). PHU is potential heat unit required for crop maturity. The range of HUI is from 0.0 at the seeding time to 1.0 at the physiological maturity.

The potential increased biomass for a day is estimated as follow:

$$\Delta B_{\mathrm{p},i} = 0.001 \cdot \mathrm{BE}_i \cdot \mathrm{PAR}_i \cdot [1 + \Delta \mathrm{HRLT}_i]^3 \tag{B21}$$

$$= 0.0005 \cdot \mathrm{BE}_i \cdot \mathrm{RA}_i \cdot [1 - \exp(-0.65 \cdot \mathrm{LAI})] \cdot [1 + \Delta \mathrm{HRLT}_i]^3 \tag{B22}$$

where ΔB_{p} is daily potential increased biomass ($\mathrm{t\,ha^{-1}}$); BE is crop parameter for converting energy to biomass ($\mathrm{kg\,ha\,m^2\,MJ^{-1}}$); HRLT and ΔHRLT are length of a day (h) and its variation ($\mathrm{h\,d^{-1}}$); PAR is intercepted photosynthetic active radiation ($\mathrm{MJ\,m^{-2}}$). RA is solar radiation ($\mathrm{MJ\,m^{-2}}$) and LAI is leaf area index, which is a function of heat units, crop stress, and crop development stages.

From emergence to the start of leaf decline, LAI is estimated with the equation:

$$\mathrm{LAI}_i = \mathrm{LAI}_{i-1} + \Delta \mathrm{LAI} \tag{B23}$$

$$= \mathrm{LAI}_{i-1} + (\Delta \mathrm{HUF})(\mathrm{LAI}_{\mathrm{mx}})(1 - \exp(5 \cdot (\mathrm{LAI}_{i-1} - \mathrm{LAI}_{\mathrm{mx}}))) \cdot \sqrt{\mathrm{REG}_i} \tag{B24}$$

HESSD
11, 9219–9279, 2014

From the start of leaf decline to the end of the growing season,

$$\mathrm{LAI}_j = \mathrm{LAI}_0 \cdot (1 - \mathrm{HUI}_j/1 - \mathrm{HUI}_0)^{\mathrm{ad}_j} \tag{B25}$$

where HUF is heat unit factor. REG is minimum crop stress factor. ad is a parameter controlled LAI decline rate for crop j and HUI_0 is HUI value when LAI begins to decline.

But the biomass growth is constrained by water, temperature, nutrient, and aeration.

$$\Delta B = \Delta B_\mathrm{p} \cdot \mathrm{REG} = \Delta B_\mathrm{p} \cdot \min(\mathrm{WS}, \mathrm{TS}, \mathrm{SN}, \mathrm{SP}, \mathrm{AS}) \tag{B26}$$

where REG is the crop growth regulating factor.

$$\text{The water stress: } \mathrm{WS}_j = \sum_{l=1}^{M} u_{j,l}/E_{\mathrm{P},j} \tag{B27}$$

$$\text{The temperature stress: } \mathrm{TS}_j = \sin[\pi \cdot (T_{\mathrm{g},j} - T_{\mathrm{b},j})/2(T_{\mathrm{o},j} - T_{\mathrm{b},j})] \quad 0 \le \mathrm{TS}_j \le 1 \tag{B28}$$

$$\text{The nitrogen stress: } \begin{cases} \mathrm{SN}_{\mathrm{S},j} = 2\left[1 - \sum_{K=1}^{i} \mathrm{UN}_K/(c_{\mathrm{NB},j} \cdot B_i)\right] \\ \mathrm{SN}_j = 1 - \mathrm{SN}_{\mathrm{S},j}/[\mathrm{SN}_{\mathrm{S},j} + \exp(3.39 - 10.93\mathrm{SN}_{\mathrm{S},j})] \end{cases} \tag{B29}$$

$$\text{The phosphorus stress: } \begin{cases} \mathrm{SP}_{\mathrm{S},j} = 2\left[1 - \sum_{K=1}^{i} \mathrm{UP}_K/(c_{\mathrm{NP},j} \cdot B_i)\right] \\ \mathrm{SP}_j = 1 - \mathrm{SP}_{\mathrm{S},j}/[\mathrm{SP}_{\mathrm{S},j} + \exp(3.39 - 10.93\mathrm{SP}_{\mathrm{S},j})] \end{cases} \tag{B30}$$

$$\text{The aeration stress: } \begin{cases} \mathrm{SAT} = \mathrm{SW1}/\mathrm{PO1} - \mathrm{CAF}_j \\ \mathrm{AS}_{\mathrm{S},j} = 1 - \mathrm{SAT}/[\mathrm{SAT} + \exp(-1.291 - 56.1 \cdot \mathrm{SAT})] \quad \mathrm{SAT} > 0.0 \end{cases} \tag{B31}$$

where T_g and T_0 are average daily soil surface temperature and the optimal temperature for crop j, respectively; SAT is saturation factor SW1 and PO1 are water content and porosity of the top 1 m of soil (mm), respectively; CAF is critical aeration factor for crop j; AS is aeration stress factor.

HESSD
11, 9219–9279, 2014

The crop yield is estimated using the harvest index, viz.:

$$\mathrm{YLD}_j = \mathrm{HI}_j \cdot B_{\mathrm{AG}} \tag{B32}$$

where YLD is total amount yield harvested from the field ($\mathrm{t\,ha^{-1}}$), and HI is harvest index; BAG is the above-ground biomass. For non-stressed conditions, harvest index increases nonlinearly from zero at seedling to HI at maturity. Affected by water stress, the harvest index is calculated as following

$$\mathrm{HIA}_i = \mathrm{HIA}_{i-1} - \mathrm{HI}_j \cdot \mathrm{WSYF}_j \cdot \mathrm{FHU}_i \cdot (0.9 - \mathrm{WS}_i)/[1 + \mathrm{WSYF}_j \cdot \mathrm{FHU}_i \cdot (0.9 - \mathrm{WS}_i)] \tag{B33}$$

where HI_j is normal harvest index of crop j; HIA is adjusted harvest index; WSYF_j is sensitivity parameter of harvest index to draught for crop j; FHU is a function of crop growth stage. The crop growth stage function is calculated as

$$\mathrm{FHU}_i = \begin{cases} \sin[\pi \cdot (\mathrm{HUI}_i - 0.3)/0.6] & 0.3 \le \mathrm{HUI}_i \le 0.90 \\ 0 & \mathrm{HUI}_i < 0.3, \mathrm{HUI}_i > 0.9 \end{cases} \tag{B34}$$

B2.2 Water use

The potential water use from surface soil to any root depth is calculated as:

$$U_{\mathrm{p},i} = E_{\mathrm{p},i} \cdot [1 - \exp(-\Lambda \cdot Z/\mathrm{RZ})]/[1 - \exp(-\Lambda)] \tag{B35}$$

The potential water use ($U_{\mathrm{p},l}$) in layer l is calculated by taking the difference between $U_{\mathrm{p},i}$ values at the layer boundaries, viz.,

$$U_{\mathrm{p},l} = E_{\mathrm{p},i} \cdot [\exp(-\Lambda \cdot Z_{l-1}/\mathrm{RZ}) - \exp(-\Lambda \cdot Z_l/\mathrm{RZ})]/[1 - \exp(-\Lambda)] \tag{B36}$$

where UP is the total water used to depth Z m on day i (mm); RZ is the root zone depth (m); Λ is a water use distribution parameter.

HESSD
11, 9219–9279, 2014
Integrated hydrological-biogeochemical system model
Y. Y. Zhang et al.

Restricted by soil water content, the potential water use (U_l) in layer l is calculated with the following equations when soil water content is less than 25 % of plant available soil water (Jones and Kiniry, 1986).

$$U_l = \begin{cases} U_{p,l} \cdot \exp[20 \cdot (SW_{l,i} - WP_l)/(FC_l - WP_l) - 1] & \text{if } SW_{l,i} < (FC_l - WP)_l/4 + WP_l \\ U_{p,l} & \text{if } SW_l \geq (FC_l - WP_l)/4 + WP_l \end{cases} \quad (B37)$$

B2.3 Nutrient uptake

The daily crop nutrient uptake (N and P) is the difference between crop nutrient demand and ideal nutrient content for day i.

$$\begin{cases} UND_i = c_{NB,i} \cdot B_i - \sum_{K=1}^{i} UN_K \\ UPD_i = c_{PB,i} \cdot B_i - \sum_{K=1}^{i} UP_K \end{cases} \quad (B38)$$

where UND and UNP are N and P uptake amount ($kg\,ha^{-1}$); UN and UP are the actual uptake of N and P; c_{NB} and c_{NP} are the optimal N and P concentration of the crop ($kg\,t^{-1}$); B is the accumulated biomass for day i ($t\,ha^{-1}$).

The NO_3-N mass flow to the roots is used to distribute potential N uptake among soil layers.

$$\begin{cases} UN_{l,i} = u_{l,i} \cdot (WNO_{3l}/SW_l)_i \\ UNS_i = \sum_{K=1}^{M} UN_{l,i} \end{cases} \quad (B39)$$

where WNO_3 is NO_3-N amount in soil ($kg\,ha^{-1}$). The total N available for uptake by mass flow UNS is estimated by summing UN of all layers.

The total P available for uptake is calculated using the equation

$$\begin{cases} UPS_i = 1.50 \cdot UPD_i \cdot \sum_{l=1}^{M} LF_{u,l} \cdot (RW_l/RWT_i) \\ LF_{u,l} = 0.1 + 0.9 \cdot c_{LP,l}/[c_{LP,l} + 117 \cdot \exp(-0.283 \cdot c_{LP,l})] \end{cases} \quad (B40)$$

HESSD
11, 9219–9279, 2014

where UPS is the amount of P supplied by soil (kg ha^{-1}); RW and RWT are the root weight in layer l and in total (kg ha^{-1}); LF_u is the labile P factor for uptake (g t^{-1}).

A portion of uptake N will be fixed by legumes, viz.,

$$\begin{cases} WFX_i = FXR_i \cdot UND_i & WFX \leq 6.0 \\ FXR = \min(1.0, FXW, FXN) \cdot FXG \end{cases} \tag{B41}$$

where FXG is the growth stage factor; FXW and FXN are the factors of soil water and NO_3-N, respectively. All of these factors are calculated using the follow equations.

$$FXG_i = \begin{cases} 0.0 & HUI_i \leq 0.15, HUI_i \geq 0.75 \\ 6.67HUI_i - 1.0 & 0.15 < HUI_i \leq 0.3 \\ 1.0 & 0.3 < HUI_i \leq 0.55 \\ 3.75 - 5.0HUI_i & 0.55 < HUI_i < 0.75 \end{cases} \tag{B42}$$

$$\begin{aligned} & FXW_i = (SW_{0.3,i} - WP_{0.3})/0.85 \cdot (FC_{0.3} - WP_{0.3}) \\ & SW_{0.3} < 0.85(FC_{0.3} - WP_{0.3}) + WP_{0.3} \end{aligned} \tag{B43}$$

$$FXN_i = \begin{cases} 0.0 & WNO_3 > 300\,\text{kg ha}^{-1}\,\text{m}^{-1} \\ 1.5 - 0.005 \cdot WNO_3/RD & 100 < WNO_3 \leq 300 \\ 1.0 & WNO_3 \leq 100 \end{cases} \tag{B44}$$

where $SW_{0.3}$, $WP_{0.3}$ and $FC_{0.3}$ are the water contents in the top 0.3 m soil, at wilting point and field capacity, respectively.

HESSD
11, 9219–9279, 2014
Integrated hydrological-biogeochemical system model
Y. Y. Zhang et al.

Appendix C: Environmental process modules

C1 Soil erosion module (SEM)

The soil erosion by precipitation is estimated using the improved ULSE equation (Onstad and Foster, 1975), viz.,

$$Y = \begin{cases} \left(0.646\mathrm{EI} + 0.45Q \cdot q_\mathrm{p}^{0.333}\right) \cdot K \cdot \mathrm{CE} \cdot \mathrm{PE} \cdot \mathrm{LS} & Q > 0. \\ 0 & Q \le 0. \end{cases} \tag{C1}$$

where Y is the sediment yield ($\mathrm{t\,ha^{-1}}$); Q is runoff volume (mm); q_p is peak runoff rate ($\mathrm{mm\,h^{-1}}$); K is soil erodibility factor determined by the soil type; PE is erosion control practice factor.

LS is the factor of slope length and steepness:

$$\begin{cases} \mathrm{LS} = (\lambda/22.1)^{\xi}(65.41S^2 + 4.56S + 0.065) \\ \xi = 0.6 \cdot [1 - \exp(-35.835S)] \end{cases} \tag{C2}$$

CE is the crop management factor:

$$\mathrm{CE} = (0.8 - \mathrm{CE}_{\mathrm{mn},j})\exp(-0.00115\mathrm{CV}) + \mathrm{CE}_{\mathrm{mn},j} \tag{C3}$$

EI is the rainfall energy factor:

$$\mathrm{EI} = R \cdot [12.1 + 8.9 \cdot (\log r_\mathrm{p} - 0.434) \cdot r_{0.5}]/1000 \tag{C4}$$

where S is land surface slope ($\mathrm{m\,m^{-1}}$) and λ is slope length (m); ξ is a parameter dependent upon slop; $\mathrm{CE}_{\mathrm{mn},j}$ is the minimum crop management factor of crop j; CV is soil cover (above ground biomass and residue) ($\mathrm{kg\,ha^{-1}}$). R is daily rainfall amount (mm) and r_p, $r_{0.5}$ is the peak rainfall rate and maximum 0.5 h rainfall intensity ($\mathrm{mm\,h^{-1}}$). The value of r_p is obtained according to the exponential rainfall distribution.

Discussion Paper | Discussion Paper | Discussion Paper | Discussion Paper |
HESSD
11, 9219–9279, 2014
Integrated hydrological-biogeochemical system model
Y. Y. Zhang et al.

C2 Mass migration module (MMM)

C2.1 N migration

The loss of NO_3-N is considered to happen only in the 10 mm depth of surface soil.

$$\begin{cases} V_{NO_3} = W_{NO_3} \cdot [1 - \exp(-QT/UL)] \\ c_{NO_3} = V_{NO_3}/QT \end{cases} \quad \text{(C5)}$$

where W_{NO_3} is NO_3-N weight in soil (kg ha^{-1}); QT is water loss in the upper layer (mm); UL is maximum soil water content (mm); V_{NO_3} is NO_3^-N loss in the soil (kg ha^{-1}) and c_{NO_3} is NO_3-N concentration in soil (g m^{-3}).

The amount of organic N migrated with the sediment is estimated using the equation

$$Y_{ON} = 0.001 \cdot Y \cdot c_{ON} \cdot \mathrm{ER} \quad \text{(C6)}$$

where Y_{ON} is loss of organic N (kg ha^{-1}); c_{ON} is organic N concentration in the upper soil layer (g m^{-3}); ER is enrich ratio.

C2.2 P migration

The loss of soluble P is estimated using the equation

$$\mathrm{YSP} = 0.01 \cdot c_{LP,l} \cdot Q/k_d \quad \text{(C7)}$$

where YSP is loss of soluble P (kg ha^{-1}); $c_{LP,l}$ is labile P concentration (g m^{-3}); k_d is ratio of total P concentration to P concentration in the runoff.

The amount of P migrated with the sediment is estimated using the equation

$$\mathrm{YP} = 0.001 \cdot Y \cdot c_P \cdot \mathrm{ER} \quad \text{(C8)}$$

where YP is loss of deposited P due to sediment migration (kg ha^{-1}); c_P is P concentration in the upper soil layer (g m^{-3}).

HESSD
11, 9219–9279, 2014
Integrated hydrological-biogeochemical system model
Y. Y. Zhang et al.

Title Page
Abstract | Introduction
Conclusions | References
Tables | Figures
◀| |▶
◀ ▶
Back | Close
Full Screen / Esc
Printer-friendly Version
Interactive Discussion

C3 Water quality module (WQM)

The basic equation of in-stream water quality module is

$$dC/dt = -KC + \sum S_{out} \tag{C9}$$

where C is the pollutant concentration ($mg\,L^{-1}$); K is the degradation coefficient and $\sum S_{out}$ is the external source items.

The equation of water quality module of water impounding is as follow.

$$\begin{cases} dh/dt = [Q_{in} - Q_{out}]/A + P - E \\ dC_L/dt = [C_{in}Q_{in} - C_L Q_{out}]/Ah - K_{set}C_L - K_d C_L + K_{scu}C_s \cdot d/h \\ dC_s/dt = h/d \cdot K_{set}C_L - K_{scu}C_s - K_{bur}C_s \end{cases} \tag{C10}$$

where h and d are water and sediment depth, respectively (m); Q_{in} and Q_{out} are inflow and outflow, respectively ($m^3\,s^{-1}$); C_{in} and C_{out} are mass fluxes into and out of the water body ($mg\,L^{-1}$); P and E are precipitation and evapotranspiration (m); C_L and C_s are constituent concentration in the water body and the sediment ($mg\,L^{-1}$); K_d, K_{set}, K_{scu} and K_{bur} are degradation and settling coefficient of pollutant in the water body, resuspension and decay coefficient of pollutant in the sediment, respectively; A is water surface area (km^2).

Appendix D: Dams regulation module (DRM)

The water balance model is used to consider inflow, outflow, precipitation, evapotranspiration and seepage of dam or sluice. The equation is:

$$\Delta V = V_{flowin} - V_{flowout} + V_{pcp} - V_{evap} - V_{seep} \tag{D1}$$

HESSD
11, 9219–9279, 2014

where ΔV, V_{flowin} and $V_{flowout}$ are daily water storage variation, daily volume of water entering and flowing out, respectively (m^3) which are calculated by hydrological process module; V_{pcp}, V_{evap} and V_{seep} are precipitation, evaporation and seepage volume, respectively (m^3), which are functions of water surface area and vary with water storage change. In the design of dam in China, there is a definite correspondence relationship among water level, storage volume and outflow. The water discharge is determined by water level or storage volume (Zhang et al., 2013).

Acknowledgements. This study was supported by the Natural Science Foundation of China (No. 41271005), the Key Project for the Strategic Science Plan in IGSNRR, CAS (No. 2012ZD003), the Endeavour Research Fellowship and China Visiting Scholar Project from China Scholarship Council. Thanks to Yongqiang Zhang and James R. Frankenberger for their comments in CSIRO internal paper review, which helped improving the quality and presentation of the manuscript.

References

Arnold, J. G., Srinivasan, R., Muttiah, R. S., and Williams, J. R.: Large-area hydrologic modeling and assessment: Part I. Model development, J. Am. Water Resour. As., 34, 73–89, 1998.

Beven, K. J. and Binley, A.: The future of distributed models: model calibration and uncertainty prediction, Hydrol. Process., 6, 279–298, 1992.

Bicknell, B. R., Imhoff, J. C., Kittle, J. L., Donigian, A. S., and Johanson, R. C.: Hydrologic Simulation Program –FORTRAN (HSPF): User's Manual for Release 10, Report No. EPA/600/R-93/174, US EPA Environmental Research Lab, Athens, Ga., 1993.

Bingner, R. L., Theurer, F. D., and Yuan, Y.: AnnAGNPS Technical Processes: Documentation Version 2, Unpublished Report, USDA-ARS National Sedimentation Laboratory, Oxford, Miss, 2001.

Bouraoui, F. and Dillaha, T. A.: ANSWERS-2000: runoff and sediment transport model, J. Environ. Eng., 122, 493–502, 1996.

Brown, L. C. and Barnwel, T. O.: The enhanced stream water quality models QUAL2E and QUAL2E-UNCAS: documentation and user manual, Env. Res. Laboratory, US EPA, 1987.

Burt, T. P. and Pinay, G.: Linking hydrology and biogeochemistry in complex landscapes, Prog. Phys. Geog., 29, 297–316, 2005.
China's national standard: (GB/T21010-2007), Current land use condition classification, 2007-08-10, 2007.
China State Environmental Protection Administration (CSEPA): Environmental quality standards for surface water – GB 3838–2002, China Environmental Science Press, Beijing, 2002 (in Chinese).
Deng, J., Zhu, B., Zhou, Z., Zheng, X., Li, C., Wang, T., and Tang, J.: Modeling nitrogen loadings from agricultural soils in southwest China with modified DNDC, J. Geophys. Res., 116, G02020, doi:10.1029/2010JG001609, 2011.
Di Toro, D. M., Fitzpatrick, J. J., and Thomann, R. V.: Water quality analysis simulation program (WASP) and model verification program (MVP)-Documentation, Hydroscience, Inc., Contract No. 68-01-3872, Westwood, NY, for US EPA, Duluth, MN, 1983.
Duan, Q., Sorooshian, S., and Gupta, V. K.: Optimal use of the SCE-UA global optimization method for calibrating watershed models, J. Hydrol., 158, 265–284, 1994.
Efstratiadis, A. and Koutsoyiannis, D.: One decade of multi-objective calibration approaches in hydrological modelling: a review, Hydrolog. Sci. J., 55, 58–78, 2010.
Gassman, P. W., Reyes, M. R., Green, C. H., and Arnold, A. G.: The soil and water assessment tool: historical development, applications, and future research directions, T. ASABE, 50, 1211–1250, 2007.
Gleick, P. H.: Water in crisis: paths to sustainable water use, Ecol. Appl., 8, 571–579, 1998.
Goldberg, D. E.: Genetic Algorithms in Search, Optimization, and Machine Learning, Addison-Wesley, Reading Menlo Park, 1989.
Grayson, R. B., Moore, I. D., and McMahon, T. A.: Physically based hydrologic modeling, 2. Is the concept realistic?, Water Resour. Res., 26, 2659–2666, 1992.
Gupta, H. V., Sorooshian, S., and Yapo, P. O.: Toward improved calibration of hydrologic models: multiple and noncommensurable measures of information, Water Resour. Res., 34, 751–763, 1998.
Hamrick, J. M.: A three-dimensional environmental fluid dynamics computer code: theoretical and computational aspects, Special Report 317, The College of William and Mary, Williamsburg ,US, 1992.
Hargreaves, G. H. and Samani, Z. A.: Estimating potential evapotranspiration, J. Irr. Drain. Div.-ASCE, 108, 225–230, 1982.

Henan Statistical Yearbook in 2003, 2004 and 2005. China Statistics Press, Beijing, China, 2003, 2004, 2005 (in Chinese).
Horst, W. J., Kamh, M., Jibrin, J. M., and Chude, V. O.: Agronomic measures for increasing P availability to crops, Plant. Soil., 237, 211–223, 2001.
Jones, C. A. and Kiniry, J. R. (Eds.): CERES-Maize, Texas A&M Univ. Press, College Station, 1986.
Jordan, Y. C., Ghulam, A., and Hartling, S.: Traits of surface water pollution under climate and land use changes: a remote sensing and hydrological modeling approach, Earth-Sci. Rev., 128, 181–195, doi:10.1016/j.earscirev.2013.11.005, 2014.
Kirchner, J. W.: A double paradox in catchment hydrology and geochemistry, Hydrol. Process., 17, 871–874, 2003.
Kindler, J.: Integrated water resources management: the meanders, Water Int., 25, 312–319, 2000.
Kennedy, J.: Particle swarm optimization, Encyclopedia of Machine Learning, Springer, US, 760–766, 2010.
Letcher, R. A., Croke, B. F. W., and Jakeman, A. J.: Integrated assessment modelling for water resource allocation and management: a generalised conceptual framework, Environ. Modell. Softw., 22, 733–742, 2007.
Li, C., Frolking, S., and Frolking, T. A.: A model of nitrous oxide evolution from soil driven by rainfall events: 1. Model structure and sensitivity, J. Geophys. Res., 97, 9759–9776, 1992.
Madsen, H.: Parameter estimation in distributed hydrological catchment modelling using automatic calibration with multiple objectives, Adv. Water Resour., 26, 205–216, 2003.
McDonnell, J. J., Sivapalan, M., Vaché K., Dunn, S., Grant, G., Haggerty, R., Hinz, C., Hooper, R., Kirchner, J., Roderick, M. L., Selker, J., and Weiler, M.: Moving beyond heterogeneity and process complexity: a new vision for watershed hydrology, Water Resour. Res., 43, W07301, doi:10.1029/2006WR005467, 2007.
Milly, P. C. D., Wetherald, R. T., Dunne, K. A., and Delworth, T. L.: Increasing risk of great floods in a changing climate, Nature, 415, 514–517, 2002.
Neitsch, S. L., Arnold, J. G., Kiniry, J. R., and Williams, J. R.: Soil and Water Assessment Tool Theoretical Documentation, Version 2005, USDA-ARS Grassland, Soil and Water Research Laboratory, Temple, Tex., 2005.
Onstad, C. A. and Foster, G. R.: Erosion modeling on a watershed, T. ASAE, 18, 288–292, 1975.

Pimentel, D., Berger, B., Filiberto, D., Newton, M., Wolfe, B., Karabinakis, E., Clark, S., Poon, E., Abbett, E., and Nandagopal, S.: Water resources: agricultural and environmental issues, BioScience , 54, 909–918, 2004.
Pushpalatha, R., Perrin, C., Le Moine, N., and Andréassian, V.: A review of efficiency criteria suitable for evaluating low-flow simulations, J.Hydrol., 420–421, 171–182, 2012.
Rallison, R. E. and Miller, N.: Past, present and future SCS runoff procedure, in: Rainfall Runoff Relationship, edited by: Singh, V. P., Water Resources Publication, Littleton, CO, 353–364, 1981.
Reichert, P. and Schuwirth, N.: Linking statistical description of bias to multi-objective model calibration, Water Resour. Res., 48, W09543, doi:10.1029/2011WR011391, 2012.
Revenga, C., Brunner, J., Henninger, N., Kassem, K., and Payne, R.: Pilot analysis of global ecosystems: freshwater systems, World Resources Institute, Washington, DC, USA, 2000.
Ritchie, J. T.: A model for predicting evaporation from a row crop with incomplete cover, Water Resour. Res., 8, 1205–1213, 1972.
Schiermeier, Q.: Increased flood risk linked to global warming, Nature, 470, 316, doi:10.1038/470316a, 2011.
Sharpley, A. N. and Williams, J. R.: EPIC-erosion/productivity impact calculator: 1. Model documentation, Technical Bulletin – United States Department of Agriculture, 1990.
Singh, V. P. and Woolhiser, D. A.: Mathematical modeling of watershed hydrology, J. Hydrol. Eng., 7, 270–292, 2002.
van Griensven, A., Francos, A., and Bauwens, W.: Sensitivity analysis and auto-calibration of an integral dynamic model for river water quality, Water Sci. Technol., 45, 325–332, 2002.
van Griensven, A., Meixner, T., Grunwald, S., Bishop, T., Diluzio, M., and Srinivasan, R.: A global sensitivity analysis tool for the parameters of multi-variable catchment models, J. Hydrol., 324, 10–23, 2006.
Vörösmarty, C. J., McIntyre, P. B., Gessner, M. O., Dudgeon, D., Prusevich, A., Green, P., Glidden, S., Bunn, S. E., Sullivan, C. A., Reidy L. C., and Davies, P. M.: Global threats to human water security and river biodiversity, Nature, 467, 555–561, 2010.
Wang, G., Xia, J., and Chen, J.: Quantification of effects of climate variations and human activities on runoff by a monthly water balance model: a case study of the Chaobai River basin in northern China, Water Resour. Res., 45, W00A11, doi:10.1029/2007WR006768, 2009.

HESSD
11, 9219–9279, 2014

Integrated hydrological-biogeochemical system model

Y. Y. Zhang et al.

Title Page
Abstract | Introduction
Conclusions | References
Tables | Figures
◀| |▶
◀ ▶
Back | Close
Full Screen / Esc
Printer-friendly Version
Interactive Discussion

Watson, N.: Integrated river basin management: a case for collaboration, International Journal of River Basin Management, 4, 243–257, 2004.
Wigmosta, M. S., Vail, L. W., and Lettenmaier, D. P.: A distributed hydrology-vegetation model for complex terrain, Water Resour. Res., 30, 1665–1679, 1994.
Wilhite, D. A.: Drought and water crises: science, technology and management issues, CRC Press, Boca Raton, US, 2005.
Xia, J.: Identification of a constrained nonlinear hydrological system described by Volterra Functional Series, Water Resour. Res., 27, 2415–2420, 1991.
Xia, J., Wang, G., Tan, G., Ye, A., and Heart, H. G.: Development of distributed time-variant gain model for nonlinear hydrological systems, Sci. China Earth Sci., 48, 713–723, 2005.
Zhang, Y., Xia, J., Shao, Q., and Zhai, X.: Water quantity and quality simulation by improved SWAT in highly regulated Huai River Basin of China, Stoch. Env. Res. Risk A, 27, 11–27, 2013.
Zhou, Y., Khu, S. T., Xi, B., Su, J., Hao, F., Wu, J., and Huo, S.: Status and challenges of water pollution problems in China: learning from the European experience, Environmental Earth Sciences, 72, 1243–1254, 2014.

HESSD
11, 9219–9279, 2014

Table 1. The widely used models and their main focuses.

Element Model	Hydrology			Environment			Ecology	
	soil water	surface water	ground water	nonpoint source	instream water quality	lake water quality	crop growth	soil biochemistry
HSPF		√		√	√	√		
SHE	√	√	√		√			
ANSWERS	√	√		√	√	√		
AnnAGNPS	√	√		√	√	√		
WASP		√			√	√		
QUAL2K		√			√	√		
EFDC		√			√	√		
DNDC		√					√	√
EPIC							√	√
BEPS							√	√
SWAT	√	√	√	√	√	√	√	√

HESSD
11, 9219–9279, 2014

Table 2. The data sets and their categories used in HE^{X}M.

Category	Data	Objectives of HE^{X}M	Controlled processes of HE^{X}M
GIS	DEM	Elevation, slopes and lengths of each sub-basin and channel	Hydrology and environment
	Land use map	Land use types and their corresponding areas in each sub-basin	Hydrology, environment and ecology
	Soil map	Soil physical properties of each sub-basin such as bulk density, texture, saturated conductivity	
Weather	Daily precipitation Daily maximum and minimum temperature	Daily precipitation of each sub-basin Daily maximum and minimum temperature of each sub-basin	Hydrology
Hydrology	Daily runoff observations	Hydrological parameter calibration	Hydrology
Environment	The outlets and the discharge data The concentration observation	Point source pollutant load Environmental parameter calibration	Environment
Ecology	Crop yield, leaf area index	Ecological parameter calibration	Ecology
Economy	The basic economic statistical indictors	Populations, GDP, breeding stock of large animals and livestock, water withdrawal in each sub-basin	Hydrology and environment
Water projects	The reservoir's design data attribute parameters	Regulation rules of reservoirs or sluices	Hydrology
Agricultural management	Fertilization time and amount, the time of seeding and harvest, crop types	Agricultural management rules of each sub-basin	Environment and ecology

HESSD
11, 9219–9279, 2014

Table 3. Sensitive parameters, corresponding ranges, and relative importance for runoff and NH_4-N simulation.

Name	Min	Max	Definition	Relative Importance for runoff (%)	Relative Importance for NH_4-N (%)
WMc	0.20	0.45	The field capacity of soil	32.73	11.10
WM	0.45	0.75	The saturated moisture capacity of soil	11.68	11.83
g_1	0	3	The basic runoff coefficient	7.30	10.34
g_2	0	3	The influence coefficient of soil moisture	10.54	12.11
KET_p	0	3	The adjustment factor of evapotranspiration	23.21	10.71
k_r	0	1	The soil runoff yield coefficient	9.55	3.20
T_g	1	100	Delay time for aquifer recharge	1.74	–
k_g	0	1	The ground runoff yield coefficient	2.91	–
f_c	0	120	The steady state infiltration rate	0.33	–
rk1	0.02	3.4	The CBOD deoxygenation rate at 20 °C	–	6.62
rk3	−0.36	0.36	The CBOD settling rate at 20 °C	–	3.60
bc1	0.1	1	The bio-oxidation rate of NH_4-N at 20 °C	–	1.97
res_set (NH_4-N)	0	100	The settling rate of NH_4-N in the reservoirs	–	14.17
res_rk1	0.02	3.4	The CBOD deoxygenation rate in the reservoirs at 20 °C	–	2.12
res_bc1	0.1	1.0	The bio-oxidation rate of NH_4-N in the reservoirs at 20 °C	–	4.51
Total relative importance				100.00	92.27

HESSD
11, 9219–9279, 2014

Integrated hydrological-biogeochemical system model

Y. Y. Zhang et al.

Table 4. Runoff simulation results of regulated and less-regulated stations (given in brackets) and the comparisons with the existing study. SWAT does not have daily results because it is calibrated at monthly scale.

Stations	Periods	Daily flow				Monthly flow: HE^{X}M(SWAT)			
		bias	*r*	NS	*f*	bias	*r*	NS	*f*
Regulated stations									
Huangqiao	Calibration	0.00	0.86	0.72	0.14	0.00 (0.05)	0.88 (0.69)	0.75 (0.40)	0.12 (0.32)
	Validation	0.05	0.61	0.23	0.40	0.05 (0.21)	0.81 (0.83)	0.52 (−0.25)	0.24 (0.54)
Mawan	Calibration	0.00	0.68	0.46	0.29	0.00 (0.05)	0.74 (0.82)	0.54 (0.66)	0.24 (0.19)
	Validation	−0.44	0.63	0.38	0.48	−0.44 (0.46)	0.79 (0.95)	0.52 (0.62)	0.38 (0.30)
Luohe	Calibration	0.00	0.84	0.70	0.15	0.00 (−0.04)	0.87 (0.94)	0.71 (0.87)	0.14 (0.08)
	Validation	−0.52	0.75	0.51	0.42	−0.52 (−0.56)	0.87 (0.81)	0.67 (0.54)	0.33 (0.40)
Zhoukou	Calibration	0.24	0.87	0.73	0.21	0.24 (0.10)	0.90 (0.94)	0.76 (0.88)	0.19 (0.12)
	Validation	0.41	0.79	0.55	0.36	0.41 (0.34)	0.91 (0.89)	0.70 (0.68)	0.26 (0.26)
Huaidian	Calibration	0.03	0.88	0.77	0.13	0.03 (−0.10)	0.91 (0.85)	0.81 (0.72)	0.10 (0.18)
	Validation	0.12	0.76	0.54	0.27	0.12 (−0.01)	0.87 (0.72)	0.70 (0.46)	0.18 (0.28)
Fuyang	Calibration	0.00	0.90	0.81	0.10	0.00 (0.03)	0.95 (0.92)	0.89 (0.84)	0.05 (0.09)
	Validation	0.14	0.88	0.76	0.17	0.14 (−0.41)	0.94 (0.85)	0.86 (0.63)	0.11 (0.31)
Yingshang	Calibration	−0.13	0.92	0.84	0.12	−0.13 (−0.34)	0.92 (0.82)	0.84 (0.61)	0.12 (0.30)
	Validation	0.16	0.87	0.74	0.18	0.16 (−0.27)	0.93 (0.85)	0.82 (0.69)	0.13 (0.24)
Less–regulated stations									
Shenqiu	Calibration	0.00	0.91	0.82	0.09	0.00 (−0.09)	0.94 (0.81)	0.88 (0.54)	0.06 (0.25)
	Validation	−0.13	0.83	0.67	0.21	−0.14 (−0.72)	0.98 (0.78)	0.94 (0.12)	0.08 (0.61)

HESSD
11, 9219–9279, 2014

Table 5. The comparison of runoff simulation results at regulated stations when the dam regulation is considered or not.

Stations	Regulated capacity (%)	Flow Event	Regulation considered				Regulation not considered				Range
			bias	*r*	NS	*f*	bias	*r*	NS	*f*	
Huangqiao	2.01	High	0.19	0.79	0.53	0.29	−0.11	0.80	0.47	0.28	0.01
		Low	−2.83	0.01	−9.89	4.90	−4.80	0.03	−17.42	8.06	−3.16
		Average	0.02	0.79	0.59	0.21	−0.36	0.81	0.51	0.35	−0.14
Mawan	0.29	High	0.09	0.67	0.45	0.32	−0.46	0.69	0.37	0.47	−0.15
		Low	–	–	–	–	–	–	–	–	–
		Average	−0.14	0.66	0.44	0.35	−1.01	0.68	0.26	0.69	−0.34
Luohe	0.26	High	−0.01	0.83	0.68	0.17	−0.42	0.82	0.54	0.35	−0.18
		Low	−1.82	0.01	−81.02	28.28	−3.96	0.02	−124.70	43.56	−15.28
		Average	−0.15	0.82	0.66	0.22	−0.68	0.82	0.51	0.45	−0.23
Zhoukou	1.31	High	0.28	0.85	0.67	0.26	−0.24	0.85	0.64	0.25	0.01
		Low	0.48	0.04	−7.91	3.45	−1.65	0.16	−20.29	7.93	−4.48
		Average	0.30	0.85	0.70	0.25	−0.41	0.86	0.63	0.30	−0.06
Huaidian	1.37	High	0.12	0.85	0.71	0.19	−0.47	0.85	0.46	0.39	−0.20
		Low	−0.35	0.06	−9.49	3.93	−2.67	0.04	−37.82	14.15	−10.22
		Average	0.06	0.86	0.73	0.16	−0.74	0.86	0.42	0.49	−0.33
Fuyang	2.21	High	0.10	0.89	0.78	0.15	−0.29	0.89	0.69	0.24	−0.09
		Low	−0.40	0.04	−6.09	2.82	−2.28	0.06	−21.54	8.59	−5.77
		Average	0.05	0.90	0.80	0.12	−0.50	0.90	0.68	0.31	−0.19
Yingshang	1.76	High	0.11	0.88	0.77	0.15	−0.35	0.88	0.68	0.26	−0.11
		Low	−0.39	0.02	−8.39	3.59	−2.49	0.00	−28.62	11.04	−7.45
		Average	0.05	0.89	0.79	0.12	−0.60	0.89	0.66	0.35	−0.23

HESSD
11, 9219–9279, 2014

Table 6. The comparison of NH_4-N simulation results between HE^{X}M and improved SWAT, and between considering dams regulation and no regulation.

Stations	Periods	Unregulated			Regulated: HE^{X}M(SWAT)		
		bias	*r*	*f*	bias	*r*	*f*
Regulated stations							
Luohe	Calibration	−0.67	0.60	0.54	−0.02 (−0.13)	0.93 (0.25)	0.05 (0.44)
	Validation	–	–	–	–	–	–
Zhoukou	Calibration	−0.56	0.38	0.59	0.29 (0.01)	0.61 (0.66)	0.34 (0.18)
	Validation	−1.35	0.66	0.85	0.27 (0.19)	0.56 (0.04)	0.36 (0.57)
Huaidian	Calibration	0.49	0.80	0.35	0.22 (0.01)	0.73 (0.42)	0.25 (0.30)
	Validation	0.22	0.51	0.36	0.02 (0.02)	0.67 (0.29)	0.18 (0.37)
Fuyang	Calibration	0.26	0.80	0.23	0.28 (0.00)	0.78 (−0.20)	0.25 (0.60)
	Validation	−0.38	0.56	0.41	−0.27 (−1.13)	0.76 (0.41)	0.26 (0.86)
Yingshang	Calibration	0.25	0.58	0.34	0.24 (−0.13)	0.79 (0.31)	0.23 (0.41)
	Validation	−0.76	0.62	0.57	−0.24 (0.49)	0.49 (0.46)	0.38 (0.51)
Less-regulated stations							
Shenqiu	Calibration	0.13	0.62	0.26	0.13 (–)	0.62 (–)	0.26 (–)
	Validation	0.16	0.41	0.37	0.16 (0.27)	0.41 (0.33)	0.37 (0.47)
Fantaizi	Calibration	0.38	0.51	0.44	0.45 (−0.01)	0.69 (0.18)	0.38 (0.42)
	Validation	−1.02	0.73	0.64	−0.62 (0.54)	0.61 (0.49)	0.51 (0.53)

HESSD
11, 9219–9279, 2014

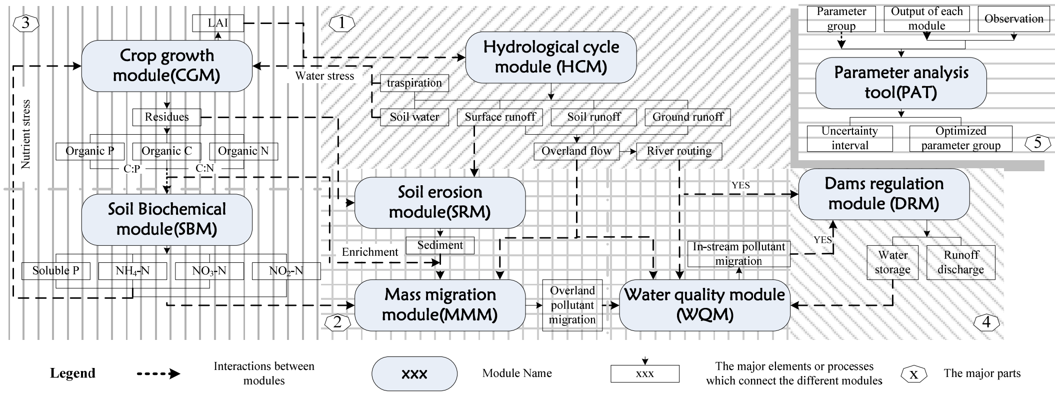

Figure 1. The structure of HE^{X}M and the interactions among the major modules (1: hydrological part; 2: environmental part; 3: ecological part; 4: dams regulation part; 5: the parameter analysis tool).

HESSD
11, 9219–9279, 2014

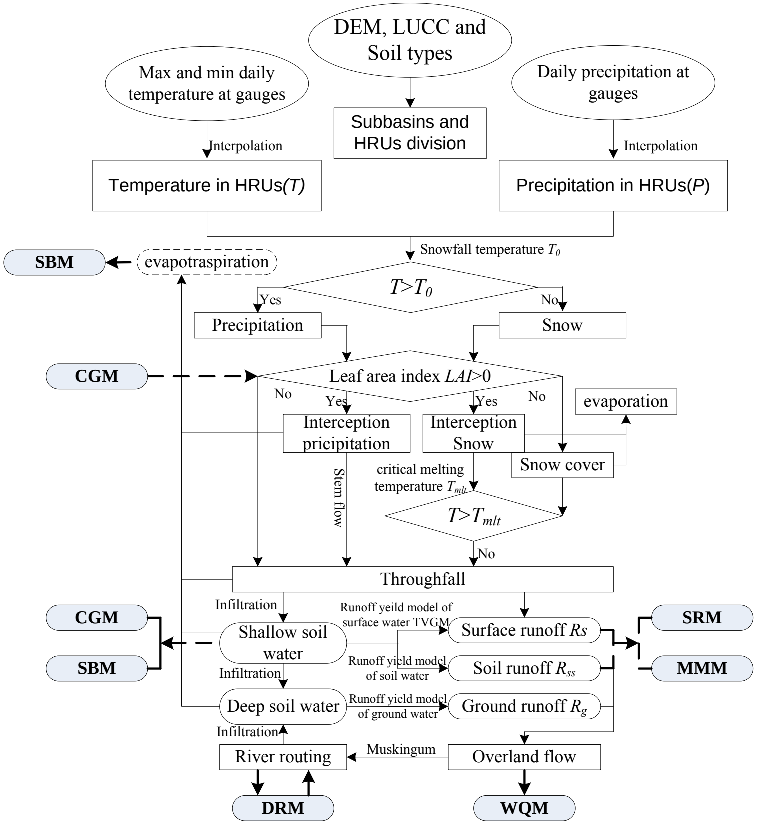

Figure 2. The flowchart of hydrological cycle module in HE^{X}M and the interactions with other modules.

HESSD
11, 9219–9279, 2014

Integrated hydrological-biogeochemical system model

Y. Y. Zhang et al.

Title Page
Abstract | Introduction
Conclusions | References
Tables | Figures
◂◂ | ▸▸
◂ | ▸
Back | Close
Full Screen / Esc
Printer-friendly Version
Interactive Discussion

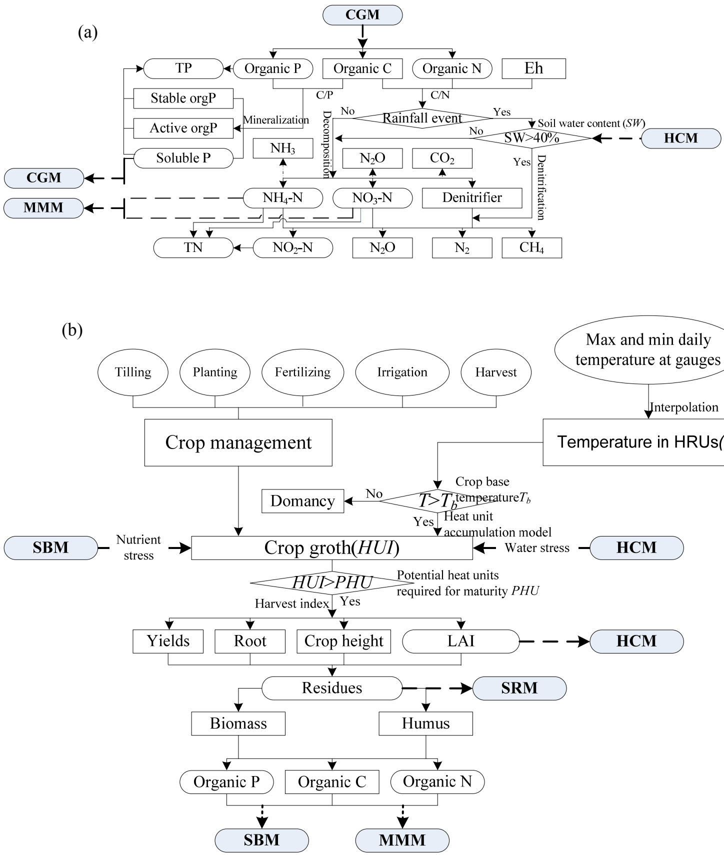

Figure 3. The flowchart of soil biochemical module **(a)** and crop growth module **(b)** in ecological part of HE^{X}M and the interactions with other modules.

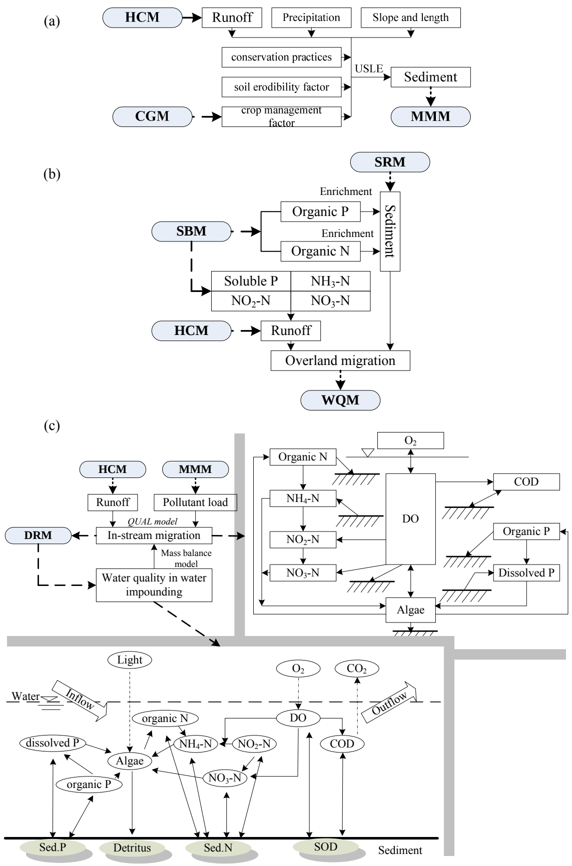

Figure 4. The flowchart of soil erosion **(a)**, mass migration **(b)** and water quality **(c)** module in environmental part of HE^{X}M and the interactions with other modules.

HESSD
11, 9219–9279, 2014

Integrated hydrological-biogeochemical system model

Y. Y. Zhang et al.

Title Page
Abstract Introduction
Conclusions References
Tables Figures
◀I ▶I
◀ ▶
Back Close
Full Screen / Esc
Printer-friendly Version
Interactive Discussion

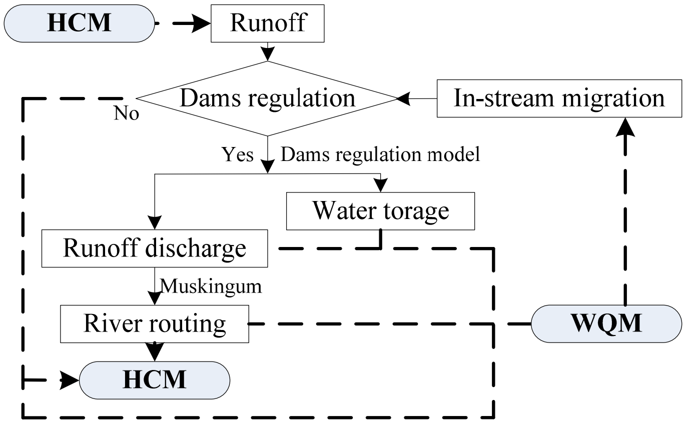

Figure 5. The flowchart of dams' regulation module in HE^{X}M and the interactions with other modules.

HESSD
11, 9219–9279, 2014
Integrated hydrological-biogeochemical system model
Y. Y. Zhang et al.

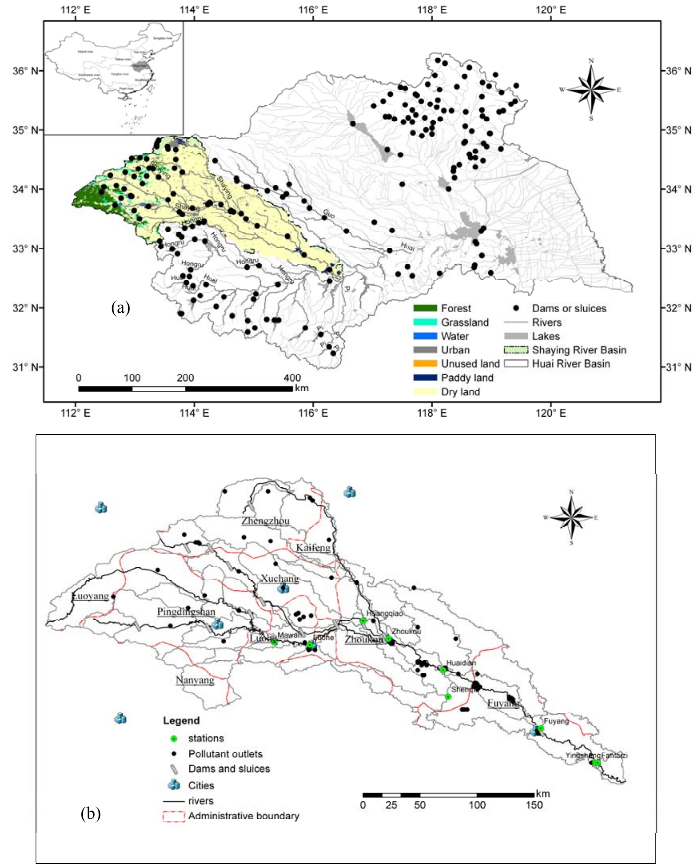

Figure 6. The location of study area **(a)** and the digital sub-basin delineation **(b)** for HE^{X}M.

HESSD
11, 9219–9279, 2014

Integrated hydrological-biogeochemical system model

Y. Y. Zhang et al.

Title Page
Abstract | Introduction
Conclusions | References
Tables | Figures
◂◂ | ▸▸
◂ | ▸
Back | Close
Full Screen / Esc
Printer-friendly Version
Interactive Discussion

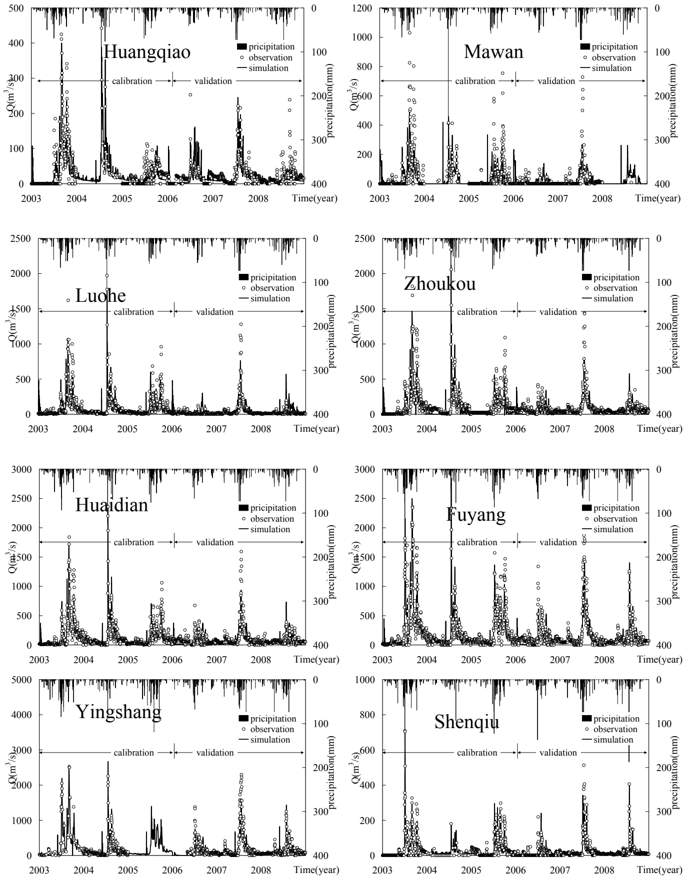

Figure 7. The daily runoff simulation at all the stations.

HESSD
11, 9219–9279, 2014

Integrated hydrological-biogeochemical system model

Y. Y. Zhang et al.

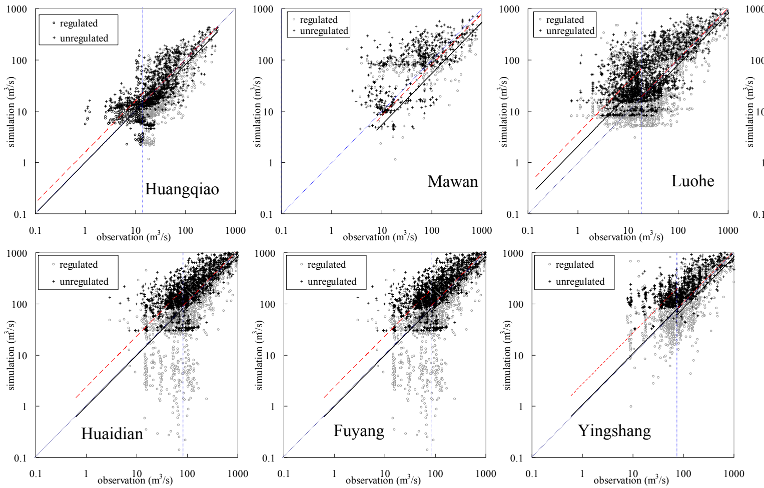

Figure 8. The comparisons between simulated and observed daily flow at the regulated stations. The results are indicated by symbols: the grey dots and red dashed trendlines for the regulated flow, the black plus signs and solid trendlines for unregulated flow. The high and low flows are separated by the vertical dashed line. The 1 : 1 line is shown as a dashed line.

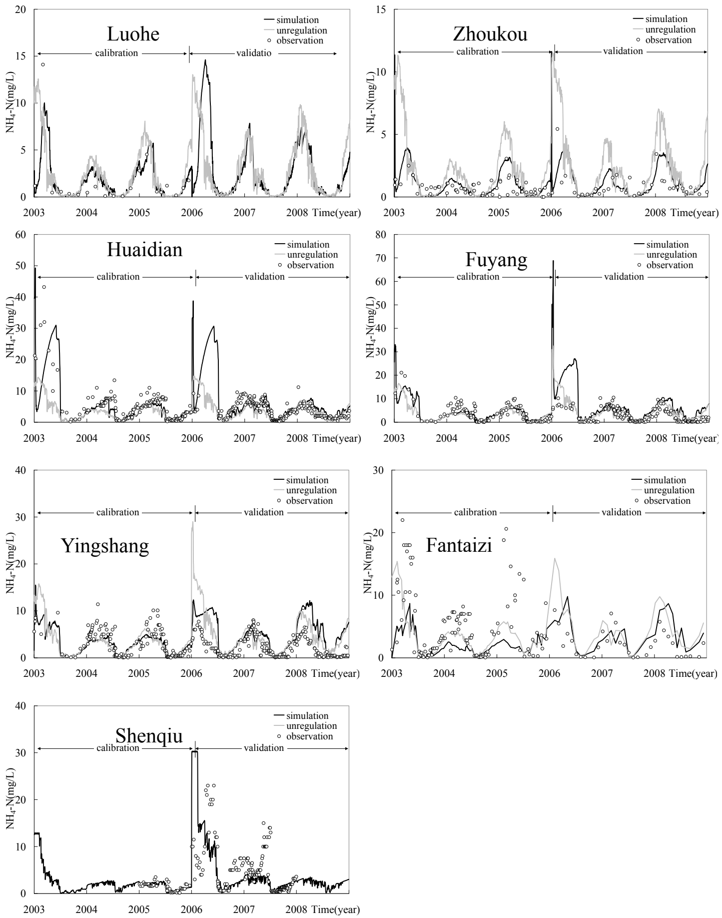

Figure 9. The simulated NH_4-N concentration variation at all the situations.

HESSD
11, 9219–9279, 2014

Integrated hydrological-biogeochemical system model

Y. Y. Zhang et al.

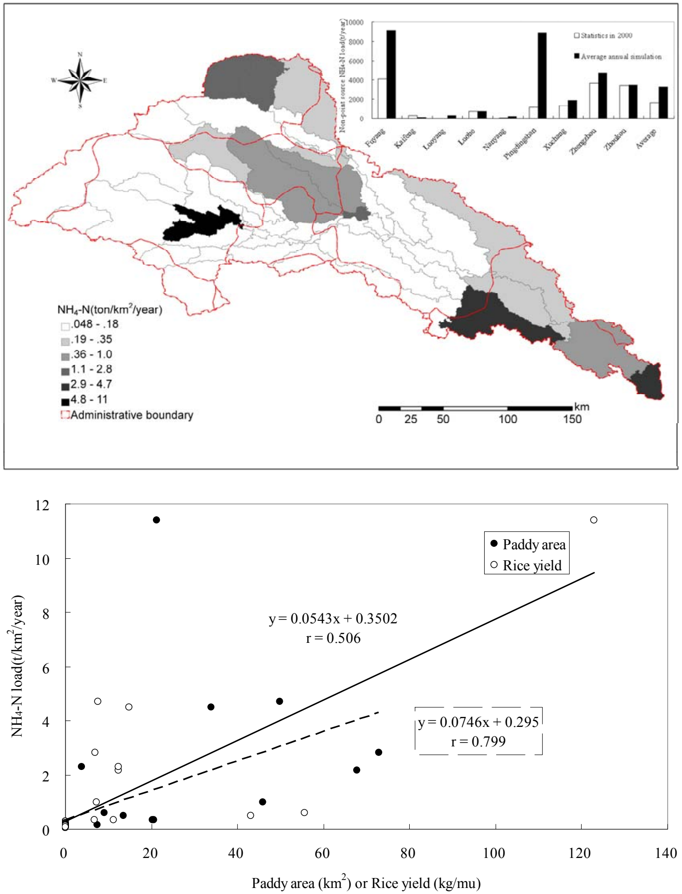

Figure 10. The spatial pattern of nonpoint source NH_4-N load and paddy area at the sub-basin scale and the city scale in Shaying River Catchment.

HESSD
11, 9219–9279, 2014

Title Page
Abstract | Introduction
Conclusions | References
Tables | Figures
◀| |▶
◀ ▶
Back | Close
Full Screen / Esc
Printer-friendly Version
Interactive Discussion

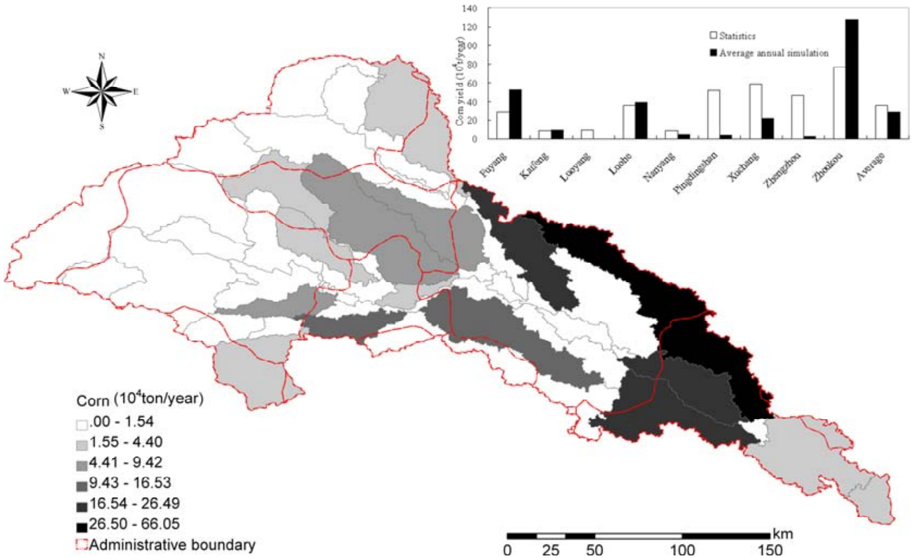

Figure 11. The spatial pattern of corn yield at the sub-basin scale and city scale in Shaying River Catchment.

HESSD
11, 9219–9279, 2014